



DESTRUCTION NOTICE

Destroy this report when it is no longer needed. DO NOT return it to the originator.

Additional copies of this report may be obtained from the National Technical Information Service, U.S. Department of Commerce, Springfield, VA 22161.

The findings of this report are not to be construed as an official Department of the Army position, unless so designated by other authorized documents.

The use of trade names or manufacturers' names in this report does not constitute indorsement of any commercial product.

UNCLASSIFIED

SECURITY CLASSIFICATION OF THIS PAGE

REPORT DOCUMENTATION PAGE

Form Approved OMB No 0704-0188 Exp. Date Jun 30, 1986

1a REPORT SECURITY CLASSIFICATION <b>Unclassified</b>		1b RESTRICTIVE MARKINGS	
2a SECURITY CLASSIFICATION AUTHORITY		3 DISTRIBUTION/AVAILABILITY OF REPORT	
2b DECLASSIFICATION/DOWNGRADING SCHEDULE			
4 PERFORMING ORGANIZATION REPORT NUMBER(S) <b>BRL-TR-2848</b>		5 MONITORING ORGANIZATION REPORT NUMBER(S)	
6a. NAME OF PERFORMING ORGANIZATION <b>Battelle Columbus Lab</b>	6b. OFFICE SYMBOL (if applicable)	7a. NAME OF MONITORING ORGANIZATION <b>US Army Research Office</b>	
6c. ADDRESS (City, State, and ZIP Code) <b>200 Park Drive, PO Box 12297 Research Triangle Park, NC 27709</b>		7b. ADDRESS (City, State, and ZIP Code) <b>PO Box 12211 Research Triangle Park, NC 27709</b>	
8a. NAME OF FUNDING/SPONSORING ORGANIZATION <b>US Army Ballistic Rsch Lab</b>	8b. OFFICE SYMBOL (if applicable) <b>SLCBR-IB-B</b>	9. PROCUREMENT INSTRUMENT IDENTIFICATION NUMBER <b>Contract DAAG29-81-D-0100</b>	
8c. ADDRESS (City, State, and ZIP Code) <b>Aberdeen Proving Ground, MD 21005-5066</b>		10. SOURCE OF FUNDING NUMBERS	
		PROGRAM ELEMENT NO.	PROJECT NO.
		TASK NO.	WORK UNIT ACCESSION NO.

11 TITLE (Include Security Classification)  
**Droplet Formation for Liquid Monopropellant Jets**

12 PERSONAL AUTHOR(S)  
**Macken, Nelson A., Swarthmore College, Swarthmore, PA 19081**

13a TYPE OF REPORT <b>TR</b>	13b TIME COVERED <b>FROM 3/17/86 TO 2/15/87</b>	14. DATE OF REPORT (Year, Month, Day)	15. PAGE COUNT
---------------------------------	--	---------------------------------------	----------------

16 SUPPLEMENTARY NOTATION  
This Scientific Services Program task was requested and funded by the Ballistic Research Laboratory.

17. COSATI CODES			18. SUBJECT TERMS (Continue on reverse if necessary and identify by block number) <b>liquid monopropellant, regenerative gun ←</b> <b>hydrodynamic jet stability,</b>
FIELD	GROUP	SUB-GROUP	

19 ABSTRACT (Continue on reverse if necessary and identify by block number)

The hydrodynamic development of droplets for conditions approximating those in the combustion chamber of regenerative liquid propellant guns has been investigated. The report contains a literature survey and discussion of various breakup mechanisms. Aerodynamic interaction is analyzed using classical stability theory and a formulation applied to anticipated working conditions. The model predicts mass removed and droplet size as a function of time. Results indicate that the jet does break up with almost all liquid atomized. Comparison to a simple burning rate model verifies that the hydrodynamic model is primarily responsible for liquid removal from the intact core. Results conflict with recent inverse gun code predictions

*She*

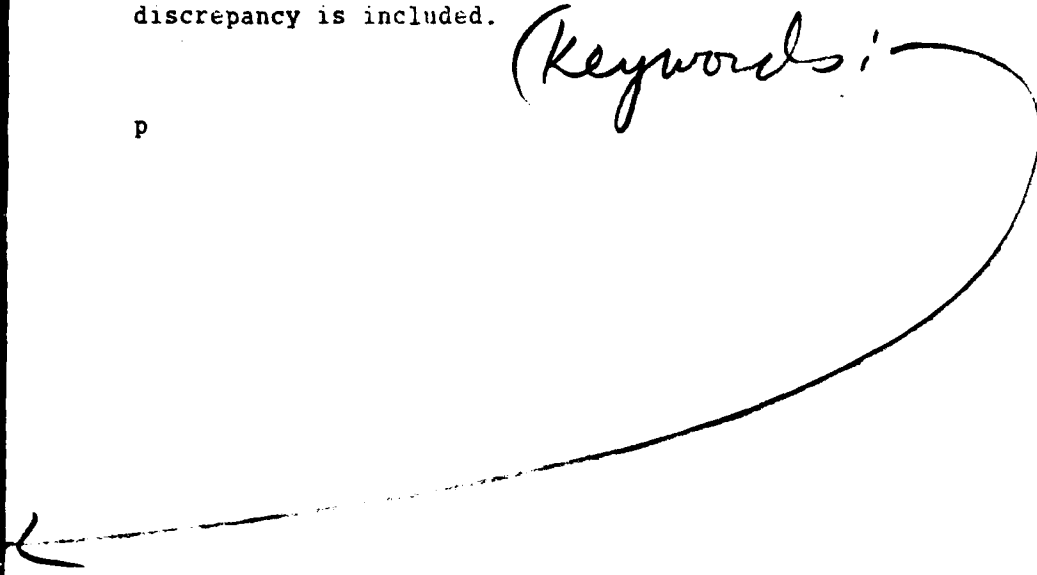
20 DISTRIBUTION/AVAILABILITY OF ABSTRACT <input checked="" type="checkbox"/> UNCLASSIFIED/UNLIMITED <input type="checkbox"/> SAME AS RPT <input type="checkbox"/> DTIC USERS		21 ABSTRACT SECURITY CLASSIFICATION <b>Unclassified</b>	
22a NAME OF RESPONSIBLE INDIVIDUAL <b>Terence P. Coffee</b>		22b TELEPHONE (Include Area Code) <b>301-278-6169</b>	22c OFFICE SYMBOL <b>SLCBR-IB-B</b>

10  
USND  
→ ABSTRACT (Con't)

which suggest significant liquid accumulation is occurring; i.e. the jet does not fully atomize and subsequently burn. A discussion of possible reasons for this discrepancy is included.

(Keywords:)

P



DROPLET FORMATION FOR LIQUID MONOPROPELLANT JETS

by

Nelson A. Macken

Swarthmore College  
Swarthmore, PA 19081

for

Ballistic Research Laboratory  
ATTN: SLCBR-IB-B (Dr. Terence P. Coffee)  
Aberdeen Proving Ground, MD 21005-5066

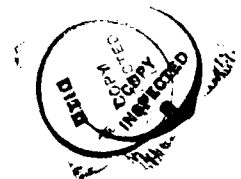
February 11, 1987

Contract No. DAAG29-81-D-0100  
Delivery Order 2089  
Scientific Services Program

The views, opinions, and/or findings contained in this report are those of the author and should not be construed as an official Department of the Army position, policy, or decision, unless so designated by other documentation.

TABLE OF CONTENTS

	<u>Page</u>
LIST OF FIGURES.....	v
1 INTRODUCTION.....	1
2 MECHANISMS FOR DROPLET FORMATION RELEVANT TO THE DESIGN OF LIQUID MONOPROPELLANT GUNS.....	2
3 ANALYSIS.....	11
4 APPLICATION OF THE ANALYSIS TO LIQUID MONOPROPELLANT JETS.....	16
5 CONCLUSIONS OF THE STUDY AND RECOMMENDATIONS FOR FUTURE ANALYSIS.....	19
REFERENCES.....	37
NOMENCLATURE.....	38
APPENDIX A.....	41
DISTRIBUTION LIST.....	53



Accession For	
NTIS CRA&I	<input checked="" type="checkbox"/>
DTIC TAB	<input type="checkbox"/>
Unannounced	<input type="checkbox"/>
Justification	
By	
Distribution /	
Availability Codes	
Date	Accession Number
A-1	

LIST OF FIGURES

<u>Figure</u>		<u>Page</u>
1	Regimes for Jet Breakup.....	25
2	Qualitative Picture of Jet Breakup.....	26
3	Jet Breakup Regime Boundaries.....	27
4	Effect of Gas Density on Jet Breakup Regime Boundaries.....	28
5	Spray Angle vs Density Ratio.....	29
6	Spray Angle vs Viscosity.....	30
7	Flow Field for Stability Analysis.....	31
8	Dispersion Relation for Second Wind Induced Breakup.....	32
9	Dispersion Relation for Second Wind Induced Breakup.....	33
10	Locus of Maximum Points of Figures 8 and 9.....	34
11	$f_m$ and $g_m$ vs. $\text{LOG}_{10} B$ .....	35
12	A Regenerative Liquid Propellant Gun with an Annular Piston.....	36

## 1. INTRODUCTION

The purpose of the reported investigation is to provide insight into liquid monopropellant jet behavior. More specifically, the mechanisms for droplet formation anticipated in the combustion chamber of existing gun designs are analyzed.

Emphasis is on hydrodynamic considerations; i.e. combustion of the liquid is not included. While this is certainly a simplification of a very complex process, it should provide insight into the details of an important consideration for droplet formation in a relatively straightforward manner.

The following chapter provides a literature survey and discussion of possible mechanisms for droplet formation. Then stability is analyzed focusing on aerodynamic interaction as the major mechanism for study. The results are applied to a typical set of gun data and a comparison is made to a parallel analysis neglecting aerodynamic interaction but assuming a uniform burning rate. A final chapter compares the results with trends indicated by other analyses and actual experimental findings. Extensions of the present work that would provide further insight are discussed.

## 2. MECHANISMS FOR DROPLET FORMATION RELEVANT TO THE DESIGN OF LIQUID MONOPROPELLANT GUNS

### 2.1 Introduction

As mentioned earlier, the focus of this study will be on droplet formation from a strictly hydrodynamic viewpoint; i.e. combustion will not be included. Therefore, droplet mechanisms that are applicable to any liquid jet can be discussed and, as expected, much information is available, ranging from simple hydrodynamic theory on falling drops to spray development in diesel engines or agricultural applications. However, very little analysis is available that pertains directly to the design of liquid monopropellant guns. In the material that follows, a description of the basic breakup regimes will be given and mechanisms for droplet formation discussed. Then typical gun data will be used to identify the regions of most interest, and various mechanisms that are applicable will be summarized.

### 2.2 Jet Breakup Regimes

Jet breakup is usually discussed in reference to a diagram of jet length vs. velocity, Figure 1, accompanied by a visual description such as Figure 2. The 'Breakup Length' in Figure 1 is the coherent portion of the liquid jet, or unbroken length. These are simplified pictures and there is even some disagreement as to the shape of Figure 1 in regions of high velocity. It is also important that Figure 1 is qualitative in nature; i.e. it is usually drawn for a certain diameter jet with given jet and surrounding properties [typically the jet is a liquid (water) and the surroundings a gas (air)].

The low velocity regions of the jet have been studied in much detail, since they are amenable to mathematical analysis. In the region of very small velocity, 'A' on Figures 1 and 2, the liquid simply drips out of the nozzle and does not form a wave at all. The linear region 'B' (Figures 1 and 2) is called the Rayleigh region, and was first described in Rayleigh's early studies on wave instability [1].\*

\* References are listed on page 23.

axisymmetric surface waves caused by surface tension, resulting in droplets with sizes larger than the jet diameter. Instability theory (discussed in more detail in the next chapter with regard to our present application) gives the wavelength for separation as:

$$\lambda = 9.02 a \quad (1)$$

where the wavelength  $\lambda$  is proportional to the droplet diameter  $d$ . (Symbols are defined in the Nomenclature). The maximum growth rate is

$$\omega_m = 0.118 \sqrt{\frac{\sigma}{\rho_1 a^3}} \quad (2)$$

The time for droplet separation is estimated as:

$$t_m = \frac{1}{\omega_m} = 8.47 \sqrt{\frac{\rho_1 a^3}{\sigma}} \quad (3)$$

The function describing the linear region was arrived at by the theory of Weber and demonstrated in the experiments of Haenlein [2]. This analysis includes the effects of viscosity as well as surface tension.

$$\frac{l}{2a} = 12 \left[ \left( \frac{2\rho_1 U_o^2 a}{\sigma} \right)^{\frac{1}{2}} + 3 \left( \frac{\mu_1 U_o}{\sigma} \right) \right] \quad (4)$$

The first dimensionless group on the r.h.s. of the above equation is the Weber number

$$We_1 = \frac{2\rho_1 U_o^2 a}{\sigma} \quad (5)$$

which is a ratio of the momentum force  $4\rho_1 U_o^2 a^2$  to the surface tension force  $(2\sigma a)$ . This particular parameter can be based on either the liquid density (as above) or the gas density, and is frequently associated with both initial jet breakup and secondary droplet breakup. Large Weber numbers would, for example, indicate that momentum forces were much larger than surface tension forces, and hence breakup would likely occur. However, there is no "critical" Weber number that will successfully predict breakup. The second dimensionless group on the r.h.s. of relationship (4) is the ratio of the Weber number to the Reynolds number.

$$\frac{\mu U_0}{\sigma} = \frac{2\rho_1 U_0^2 a}{\sigma} = \frac{We}{Re} \quad (6)$$

The Reynolds number is the ratio of the momentum force  $4\rho_1 U_0^2 a^2$  to the viscous force  $2\mu_1 U_0 a$  and is generally used to characterize laminar and turbulent flow of viscous fluids. The ratio of the two is then characteristic of the ratio of viscous forces ( $2\mu_1 U_0 a$ ) to surface tension forces ( $2\sigma a$ ). Since viscous forces are always important for high speed jet breakup, this parameter will be important in our study. High values will indicate dominance of viscous forces over surface tension forces and vice versa.

Weber's contributions to the linear breakup region also provide corrections to relationships (1), (2), and (3) which account for the effect of fluid viscosity. The wavelength of separation is given by:

$$\lambda = 8.89 a \left[ 1 + \frac{3\mu}{\sqrt{2a\rho_1\sigma}} \right] \quad (7)$$

The maximum growth rate is given by:

$$\omega_m = \left[ \sqrt{\frac{8\rho_1 a^3}{\sigma}} \quad \frac{6\mu_1 a}{\sigma} \right] \quad (8)$$

and the time for droplet separation is given by:

$$t_m = \frac{1}{\omega_m} = \sqrt{\frac{8\rho_1 a^3}{\sigma}} + \frac{6\mu_1 a}{\sigma} \quad (9)$$

In a further analysis, Weber included the pressure effects of an inviscid surrounding [3]. This predicted a maximum in the breakup region and the existence of region C (see Figures 1 and 2). Weber indicated that aerodynamic forces tend to propagate both symmetric and transverse disturbances, leading to shorter breakup lengths. The regime in which these aerodynamic forces tend to dominate is called the first wind-induced regime. This regime was also studied in more detail by Grant and Middleman [4]. They altered Weber's theory to produce a better fit to experimental data and also studied the

turbulent region, shown as 'D' in Figures 1 and 2. In the turbulent region, viscous forces tend to stabilize the jet (in terms of breakup length). Here breakup occurs in the form of ligaments of various sizes.

As the velocity is further increased, theory becomes less appropriate, and the jet definition less clear. Eventually atomization becomes more dominant and the jet breakup length is reduced. The word "atomization" was probably introduced in 1875 by Commander Isherwood of American Navy, who made a study of oil burning for naval purposes [5]. Atomization shall be referred to here as the formation of small droplets taking the shape of a conical spray (in the case of a round jet). This formation begins at the end of the jet in region D and approaches the outlet of the nozzle as the jet length is reduced in region E, called the second wind-induced regime in Figure 1. At full atomization (region F), the spray begins at the nozzle exit, although there is evidence that a liquid core still exists. The terminology "primary" as well as "secondary" atomization is also sometimes used. The former refers to the droplet formation process (the focus of this study), and the latter refers to the disintegration of previously formed droplets.

### 2.3 Additional Factors Contributing to Jet Breakup

The representation given by Figure 1 is much too simplified. An alternate way to look at flow regimes is to consider the Ohnesorge number:

$$Oh = \frac{\mu_1}{\sqrt{2\rho_1 \sigma a}} \quad (10)$$

This relationship is the square root of the Weber number divided by the Reynolds number and hence is independent of the velocity but includes both surface tension and viscosity. Some jet regime boundaries are indicated by a plot of this relationship vs. Reynolds number as in Figure 3 [6]. The Ohnesorge number was also used by Grant and Middleman to predict the maximum in the laminar breakup curve [4].

In Figure 3, the solid straight line to the immediate right of the region denoted as the Rayleigh regime is the beginning of the first wind-induced regime, region C on Figure 1. The lines marked "Ohnesorge" and "Miesse" indicate the beginning of atomization. The word "atomization" is used in the literature to denote several classes of jet breakup, and it is not clear whether the intent here is to describe a boundary for region E or F on Figure 1. The dashed lines are intended to show the effect of gas density. There is a shift in the wind-induced and atomization boundary to lower Reynolds numbers as the gas is compressed. (Other lines are for atmospheric pressure).

The effect of gas density has been discussed by others in more detail. Ranz [7] characterized sprays by using the Weber number based on gas density, among other parameters, where:

$$We_2 = \frac{2\rho_2 U_o^2 a}{\sigma} \quad (11)$$

Sterling and Sleicher [8] also proposed a relation between the Weber number and Ohnesorge number as a boundary between the Rayleigh and first wind-induced regime. Reitz [9] has summarized these effects in Figure 4 where regime boundaries are indicated as a function of density ratio, Weber number, and velocity. As expected, atomization is more likely to occur as gas density increases due to the stronger aerodynamic forces (momentum forces of the gas).

The curves on Figure 4, as on Figure 3, indicate proposed boundaries between the Rayleigh, wind-induced, and atomization regimes. (Note the gas Weber number is given by  $We_g$  rather than  $We_2$ ). Ranz [7] proposed that wind-induced jet breakup (presumably regions C and D on Figure 1) are bounded by

$$.4 < We_2 < 13$$

with atomization where

$$We_2 > 13$$

The boundary between the Rayleigh regime and first wind-induced regime (Regions B and C in Figure 1) was proposed by Sterling and Streicher [8] to be given by

$$We_2 = 1.2 + 3.4 Oh^{.9}$$

(Note that Oh is given by Z on Figure 4). Miesse [6] proposed the onset of atomization (beginning of region E) to be given by

$$We_2 = 40.3.$$

Another important factor influencing jet breakup is nozzle design, and the easiest parameter to quantify in this regard is the length-to-diameter ratio ( $L/2a$ ). Reitz and Bracco [10] have reported results of this effect, as well as that of density ratio, on jet breakup. They studied several nozzle designs, operating conditions, and working fluids, and arrived at semi-empirical correlations for spray angle, core length, and droplet size. The spray angle for the atomization region is given by:

$$\tan \frac{\theta}{2} = \frac{4\pi}{A} f \left( \frac{\rho_1}{\rho_2} \left( \frac{\sigma}{U_0 \mu_1} \right)^2 \right) / \sqrt{\frac{\rho_1}{\rho_2}} \quad (12)$$

The function 'f' is found from stability theory and will be discussed in the next chapter. It is illustrated on Figure 11. The constant 'A' is determined empirically. For their range of experiments, Reitz and Bracco [10] found A to be given by the equation:

$$A = 3 + \frac{L/2a}{3.6} \quad (13)$$

Data are presented for spray angle and two limiting cases considered. In the first case, the density ratio (liquid to gas) is high and the viscous forces are small; i.e.

$$\frac{\rho_1}{\rho_2} \left( \frac{\sigma}{\mu_1 U_0} \right)^2 \gg 1 \quad (14)$$

For this situation, Figure 5 shows spray angle as a function of nozzle design and density ratio. The design curves represent equation (12) with the value of A chosen to provide the best fit for all the data for a particular nozzle. Only a few data points are shown. The "goodness of fit" is a measure of the validity of equation (12). The 'K' curve is a semi-empirical relation showing the demarcation between atomization at the nozzle and atomization downstream of the nozzle. In Figure 1, this corresponds to the division between region E and region F. The region above the 'K' curve represents fully atomized flow. As indicated before (see Figure 4), as the gas density approaches that of the liquid, the jet is more likely to fully atomize.

The second limiting case is for more viscous flows where

$$\frac{\rho_1}{\rho_2} \left( \frac{\sigma}{\mu_1 U_0} \right)^2 \ll 1 \quad (15)$$

These results are found in Figure 6. Once again, a 'K' curve is given and the region above the curve represents full atomization. As mentioned earlier, viscosity tends to stabilize the jet.

Note that the nozzle design curves indicate that equation (12) is not as accurate for the more viscous flows (Figure 6 as compared to Figure 5).

There are other factors that influence jet behavior in addition to the fluid properties, aerodynamic effects, and nozzle geometry given by the L/2a ratio. These are discussed in detail by Reitz [9] and are related to nozzle design, fluid supply conditions, and the physical rearrangement of the flow as it leaves the nozzle. If the nozzle has a sharp inlet, the flow may not attach to the nozzle wall. This gives a more stable jet than one which reattaches, since the latter is more turbulent due to cavitation. If the flow leaving the nozzle is laminar, its profile is, of course, less uniform than if it were turbulent. It is postulated that the redistribution of energy as the flow adjusts to the removal of the nozzle produces radial velocities that contribute to jet breakup. There is some experimental evidence that fully developed turbulent jets (in the nozzle) are more stable than laminar ones. In any flow, the abrupt change in boundary

conditions leaving the nozzle affects the tangential stresses and could produce short wavelength surface waves that promote atomization. Finally, liquid supply pressure oscillations, which are commonly found in practical fuel injection systems can also have an effect on jet breakup.

#### 2.4 Factors Affecting Droplet Formation in Liquid Monopropellant Guns

Many of the above mechanisms relate to droplet formation in liquid monopropellant guns. To isolate the problem somewhat, several key variables can be computed for "typical" gun data. In this stage of development, "typical" refers to test data which are currently being compared to various analytical models. Data are given in Table 1 for the first few milliseconds of such a test. Parameters computed include  $L/2a$ , the Reynolds number, Weber numbers, the Ohnesorge number, the density ratio, and the atomization parameter in equations (14) and (15); i.e.

$$\frac{\rho_1}{\rho_2} \left( \frac{\sigma}{\mu_1 U_o} \right)^2 \quad (16)$$

For comparison purposes, figures previously presented all represent particular fluids and nozzle designs but, of course, those with dimensionless groups are somewhat more useful than others. The high Reynolds numbers ( $> 10^4$ ) and low Ohnesorge numbers indicate the probability of atomization, upon referral to Figure 3. Even though Figure 4 is for water jets into air, the extremely large Weber numbers indicate liquid breakup is probable. The values of the density ratios and abscissa of Figure 6 (also tabulated) indicate possible spray formation when compared to Figure 5. The  $L/2a$  ratios are similar but the specific nozzle designs are quite different. Also, although spray formation is evident, it is not clear whether it begins at the nozzle exit or further downstream.

The data do support evidence of atomization and hence legitimize further study. The analysis that follows does consider only aerodynamic effects and

is applicable to fluid breakup anywhere this mechanism is dominant. Since we are clearly not in a regime dominated by capillary forces, this seems feasible. However, it is quite clear that mechanisms due to nozzle design, fluid supply conditions, and the physical rearrangement of the flow are not considered. The first two of these are simply not amenable to analysis, since there is no experimental or analytical data on flow inside the nozzle itself. The third could be considered, but such rearrangement would augment droplet development. Preliminary indications are that the aerodynamic theory overestimates the amount of flow in droplet form, and inclusion of this mechanism would only exacerbate this situation; i.e. any additional mechanism considered beyond that in the next chapter should be flow stabilizing and not destabilizing.

### 3. ANALYSIS

In the analysis that follows, it will be assumed that breakup occurs because of instabilities developed in a liquid jet caused by aerodynamic forces. The procedure is outlined by Reitz [9] and Reitz & Bracco [10] with details given in the analyses of Levich [11] and Taylor [12]. For the analysis an axisymmetric cylindrical jet will be considered. Results will be applied to a geometry resembling that of a liquid monopropellant gun.

The linearized Navier-Stokes equations for the small axisymmetric fluctuating (perturbation) velocities  $u_i$ ,  $v_i$ , and pressures  $p_i$  ( $i = 1$  for liquid,  $i = 2$  for gas) are:

$$\frac{\partial u_i}{\partial z} + \frac{1}{r} \frac{\partial}{\partial r} (rv_i) = 0, \quad (1)$$

$$\begin{aligned} \frac{\partial u_i}{\partial t} + U_i(r) \frac{\partial u_i}{\partial z} + v_i \frac{dU_i}{dr} \\ = - \frac{1}{\rho_i} \frac{\partial p_i}{\partial z} + v_i \left[ \frac{\partial^2 u_i}{\partial z^2} + \frac{1}{r} \frac{\partial}{\partial r} \left( r \frac{\partial u_i}{\partial r} \right) \right], \end{aligned} \quad (2)$$

$$\begin{aligned} \frac{\partial v_i}{\partial t} + U_i(r) \frac{\partial v_i}{\partial z} \\ = - \frac{1}{\rho_i} \frac{\partial p_i}{\partial r} + v_i \left[ \frac{\partial v_i}{\partial z^2} + \frac{\partial}{\partial r} \left( \frac{1}{r} \frac{\partial}{\partial r} rv_i \right) \right] \end{aligned} \quad (3)$$

Symbols are further defined in the Nomenclature. Assuming the surface wave elevation  $\eta \ll a$ , the boundary conditions to a first order approximation can be written as (see Figure 7):

$$v_i = \frac{\partial \eta}{\partial t} + U_i \frac{\partial \eta}{\partial z}, \quad (4)$$

$$\frac{\partial u_i}{\partial r} = - \frac{\partial v_i}{\partial z}, \quad (5)$$

$$- p_1 + 2\mu_1 \frac{\partial u_1}{\partial z} - \frac{\sigma}{a^2} \left( \eta + a^2 \frac{\partial^2 \eta}{\partial z^2} \right) + p_2 = 0 \quad (6)$$

Solutions are obtained by introducing a velocity potential  $\phi$ , and stream functions  $\psi_1, \psi_2$  of the form

$$\phi_1 = \phi_1(r)e^{ikz + \omega t}, \quad (7)$$

$$\psi_1 = \Psi_1(r)e^{ikz + \omega t}, \quad (8)$$

$$\psi_2 = [U_2(r) - i(\omega/k)] C_3 e^{ikz + \omega t} f(r) \quad (9)$$

Substitution of (7) and (8) into equations 1-3 for the liquid component yields a solution in the form of modified Bessel functions  $I_n$ :

$$\phi_1 = C_1 I_0(kr), \quad (10)$$

$$\Psi_1 = C_2 r I_1(lr), \quad (11)$$

$$l^2 = k^2 + \omega/v_1 \quad (12)$$

For the gas component, an Orr-Summerfield equation for  $f(r)$  is solved to give the gas pressure:

$$p_2 = -\rho_2 \left( U_0 - i \frac{\omega}{k} \right)^2 k \frac{K_0(ka)}{K_1(ka)} \eta_0 e^{ikz + \omega t}, \quad (13)$$

where the  $K_n$  are Bessel functions of the second kind.

The constants  $C_1, C_2, C_3$  are solved for by considering the boundary conditions equations 4-6. This results in the following dispersion relationship:

$$\begin{aligned} \omega^2 + 2v_1 k^2 \omega \left( \frac{I_1'(ka)}{I_0(ka)} - \frac{2kl}{k^2 + l^2} \frac{I_1(ka)}{I_0(ka)} \frac{I_1'(la)}{I_1(la)} \right) \\ = \frac{\sigma k}{\rho_1 a^2} (1 - a^2 k^2) \left( \frac{l^2 - k^2}{l^2 + k^2} \right) \frac{I_1(ka)}{I_0(ka)} \\ + \frac{\rho_2}{\rho_1} \left( U_0 - \frac{i\omega}{k} \right)^2 k^2 \left( \frac{l^2 - k^2}{l^2 + k^2} \right) \frac{I_1(ka) K_0(ka)}{I_0(ka) K_1(ka)} \end{aligned} \quad (14)$$

where the prime denotes differentiation. The above equation relates growth rate  $\omega$  to wavelength  $\lambda$ , but is not easily solved. A limiting solution for  $ka \rightarrow \infty$  (small wavelength disturbances) where the droplet size,  $r \sim \lambda$ , is small is applicable to atomization. In this case the Bessel functions in (14) can be replaced by their asymptotic values, and (14) becomes:

$$\begin{aligned}
 & (\omega + 2\nu_1 k^2)^2 + \sigma k^3 / \rho_1 - 4\nu_1^2 k^3 (k^2 + \omega / \nu_1)^{\frac{1}{2}} \\
 & + (\omega + iU_0 k)^2 (\rho_2 / \rho_1) = 0
 \end{aligned} \tag{15}$$

This equation was arrived at independently by Levich (see his equation 125.17) for the case of high velocity jet breakup and short wavelengths, and by Taylor (see his equation 16) for ripples formed on an infinite viscous liquid. This is expected, since for  $kr \rightarrow \infty$  curvature effects would be unimportant; i.e. note (15) above is independent of  $r$ . Taylor considered a further simplification assuming:

$$\rho_2 / \rho_1 \ll 1 \tag{16}$$

In our case,  $\rho_2 / \rho_1 \sim .014$  to  $.13$ . Taylor separated equation (15) above into real and imaginary components. With assumption (16), he obtained for the real part of the disturbance growth rate,  $\omega$ :

$$\omega = 2 \frac{U_0^3}{\sigma} \left[ \frac{\rho_2^3}{\rho_1} \right]^{\frac{1}{2}} g(B, x) \tag{17}$$

where  $B$  is the droplet formation parameter:

$$B = \frac{\rho_1}{\rho_2} \left( \frac{\sigma}{\mu_1 U_0} \right)^2, \tag{18}$$

$x$  is the wavelength parameter:

$$x = \frac{\rho_2 U_0^2}{\sigma k}, \tag{19}$$

and  $g$  is given as a function of  $x$  on Figures 8 and 9.

Note that the droplet formation parameter has also been used to predict the onset of atomization (see equations 14 and 15 in Chapter 2).

Waves identified with a growth rate described by relation (17) are unstable. Separation into drops occurs for a maximum value of  $g$ ; i.e.

$$g(B, x) = g_m(B, x_m) \tag{20}$$

where  $g_m$  and  $x_m$  define the values of  $\omega$  and  $k$  for the wave that forms a drop. Figures 8, 9, 10, and 11 show the location of these maxima. Note the shift

to longer wavelengths (larger  $x$ ) with smaller values of  $B$ . Increasing  $x$  means decreasing  $k$  and increasing wavelength since:

$$k = 2\pi/\lambda \quad (21)$$

This shows that highly viscous flow, giving smaller  $B$ , leads to longer waves and less viscous flow produces shorter waves. In our case  $B$  can range from an order of magnitude of 20 to .001 with much of the data having values less than 1.

A wave of small amplitude grows on the surface until the crest is detached and a drop is formed. The diameter of the drop can be associated with the wavelength of this detached wave:

$$d = C \lambda_m \quad (22)$$

In this analysis, the simplification will be made that the constant  $C = 1$ .

As mentioned above,  $\lambda_m$  is associated with  $x_m$  since:

$$\lambda_m = 2\pi/k_m \quad (23)$$

The growth rate  $\omega$  is used to estimate the amount of time required to form a drop. During a time:

$$t_m = \frac{1}{\omega_m} \quad (24)$$

the maximum wave grows by an amount

$$e^{\omega_m \left(\frac{1}{\omega_m}\right)} = e$$

A reasonable estimate for the time to form a drop is a value proportional to  $t_m$  and, in this analysis, the proportionality constant will be considered unity.

The mass of fluid detached from unit area of the surface can be written as

$$\frac{\rho_l \pi D d \ell \lambda_m}{\pi D d \ell} = \rho_l \lambda_m \quad (25)$$

where  $dl$  is a differential length of the jet and  $D$  is the diameter of the jet (in our case the diameter of the bolt plus twice the jet thickness).

The mass detached per unit area per unit time is:

$$\dot{m} = \rho_1 \frac{\lambda_m}{t_m} \quad (26)$$

Combining equations (19) and (21) yields:

$$\lambda_m = \frac{2\pi}{k_m} = \frac{2\pi\sigma x_m}{\rho_2 U_o^2} \quad (27)$$

where the subscripts  $m$  again refer to maximum values; i.e. the values corresponding to drop formation. Equations (17) and (24) combine to get the time for drop formation.

$$t_m = \left\{ \frac{2 U_o^3}{\sigma} \left[ \frac{\rho_2^3}{\rho_1} \right]^{\frac{1}{2}} g_m (B, x_m) \right\}^{-1} \quad (28)$$

Equations (26), (27), and (28) combine to give the detached mass per unit time, per unit area, as:

$$\dot{m} = 4\pi\rho_1 U_o \left( \frac{\rho_2}{\rho_1} \right)^{\frac{1}{2}} f_m \quad (29)$$

where

$$f_m = x_m g_m (B, x_m) \quad (30)$$

Figure 11 shows  $f_m$  as a function of  $B$ .

#### 4. APPLICATION OF THE ANALYSIS TO LIQUID MONOPROPELLANT JETS

The geometry of the regenerative liquid propellant gun is shown in Figure 12. Upon firing, the annular piston compresses the fluid in the propellant chamber which is then released into the combustion chamber via the annular gap created between the piston and the stationary control rod, or bolt. The jet is annular in shape and is partially adjoined on its inside surface by the bolt.

##### 4.1 Reduction of the Analysis to Computer Code

From the previous chapter, the relationship for mass removed from the jet per unit surface area and time is: [see equation (29) from Chapter 3].

$$\dot{m} = 4 \pi \rho_1 U_0 \left( \frac{\rho_2}{\rho_1} \right)^{\frac{1}{2}} f_m \quad (1)$$

At any instant in time, there is a certain surface area of liquid remaining intact in the combustion chamber.

In actual determination of the mass removed, two models were used. The first was discrete in formulation. Over an increment of time,  $dt$ , the jet length is:

$$dl = U_0 dt \quad (2)$$

and the surface area is:

$$2 \pi D dl \quad (3)$$

To get the mass removed during time  $dt$ , combining equations (1) through (3) yields:

$$m = \left[ 4 \pi \rho_1 U_0 \left( \frac{\rho_2}{\rho_1} \right)^{\frac{1}{2}} f_m \right] 2 \pi D dl dt \quad (4)$$

During the next time increment, this amount of mass is again reduced (the velocity used in equation (4) is now the velocity at the present

time). Also, a new amount of mass has entered and part of the new amount has been removed. The mass removed is distributed into droplets with diameter given by relation (27) in Chapter 3, or:

$$\lambda_m = \frac{2\pi \sigma x_m}{\rho_2 U_0^2} \quad (5)$$

where the values of  $x_m$  and  $U_0$  are evaluated at the current time. An inventory gives the mass removed, the number and size of droplets, and the liquid remaining in the intact core at any time.

The second model used to determine the mass removed was continuous in nature. Equation (1) above was multiplied by an appropriate surface area and integrated using an o.d.e. solver. The appropriate area was considered to be that of a hollow frustrum with inner diameter equivalent to that of the bolt and outer diameter equal to the bolt plus two annuli. The height of the frustrum then corresponds to the length of the intact core. Equation (5) was again used to determine the droplet diameter, and the mass and surface area of droplets removed were computed.

The computer programs for both methods of analysis are given in the Appendix. The discrete method has more physical appeal, but the continuous model is one which can be easily incorporated as an integral part of existing gun codes, and hence satisfies the requirement for this project.

#### 4.2 Consideration of Mass Removal by Burning (Combustion)

Although the thrust of this analysis is hydrodynamic in nature, the models mentioned above can be altered to consider combustion as the major mechanism for mass removal from the liquid core. Such an analysis could be used to test the magnitude of the two effects; i.e. if the mass is removed more quickly by combustion, then perhaps hydrodynamics are not important, and vice versa. The discussion also pertains only to initial mass removal; i.e. mass could be removed hydrodynamically, form drops, and the drops

subsequently burned. The combustion model incorporates a simple burning rate relation [13]:

$$\text{Burning Rate (cm/s)} = 1.64 (\text{Pressure in MPa})^{.103} \quad (6)$$

The above can be applied to the surface area of the liquid jet, and the amount of mass removed by burning can then be determined at any time.

#### 4.3 Application of the Analysis to Actual Experimental Gun Conditions

The analysis has been applied to data computed from an existing lumped model code which predicts relative liquid velocity, area of the annulus, liquid and gas densities, and pressure as a function of time [13]. This information provides an input to the computer codes given in the Appendix. Tables 2 and 3 illustrate the results for approximately the first 2.5 milliseconds of liquid entry into the combustion chamber. In the table, the time is in milliseconds, the mass in grams, the length in cm, and the area in  $\text{cm}^2$ . Table 2, which illustrates the results using the continuous approach, shows that about 97% of the mass is atomized after about 2.5 milliseconds, a short liquid core of about .5 cm remains, and about  $4.6 \times 10^5 \text{ cm}^2$  of surface area is formed by the droplets. The discrete approach, shown in the first four columns of Table 3, shows very similar results. Differences occur because of the nature of the models. Results of the combustion analysis are also given. Note that very little mass (less than 1%) is removed by burning. This seems to indicate that mass removal by aerodynamic forces is a much more dominant mechanism than mass removal by burning.

## 5. CONCLUSIONS OF THE STUDY AND RECOMMENDATIONS FOR FUTURE ANALYSIS

The results of the analysis, when applied to the liquid monopropellant jet, indicate that the flow regime is in the atomization region and, if data from a gun code representing relative velocity, annulus area, and fluid densities are used in the stability analysis, liquid is stripped from the jet by aerodynamic forces, presumably forming drops. This mechanism has been shown to be much more dominant than the combustion process based on a simple burning rate model.

Studies at the Ballistics Research Laboratory have used experimental data in an "inverse code". By neglecting energy losses and using actual measurements, the amount of liquid reacting in the combustion chamber can be evaluated. When this is compared with the amount of liquid that has entered the chamber (also found by measurement and conservation of mass), it is inferred that there is substantial liquid accumulation; i.e. unburned liquid is present in the combustion chamber. From this result one would suspect that droplets have not formed, since if they had formed, they would presumably have burned and liquid would not have accumulated.

This presents a dilemma which bears further investigation. Some possible explanations are discussed below (there are no doubt more that perhaps are not as obvious).

The analysis presented in Chapter 3 could be incorrect when applied to the present situation. There are several possible reasons for this. The model strictly holds for round jets, not jets adjoined by a wall as is the case here; i.e. the geometry is not consistent with the model. The model also is inexact in other ways, most noticeably in the fact that it is for density ratios that are much less than one (a term containing  $\rho_2/\rho_1$  is actually dropped in the analysis). Combustion is also neglected. Although this was considered separately in a simplistic way, no attempt was made to combine the two effects.

It is also possible that the jet does break up, but does not form droplets and burn. Ligaments may be torn from the jet and they may fall or strike other portions of the chamber, perhaps even coalescing. The analysis also is not very exact when it comes to droplet size. Some ligaments could be longer than others, and constants taken in the theory to be unity could, in fact, have almost any value. If there is not substantial increase in surface area, burning could proceed slowly (the burning analysis actually showed this in the limiting case of no droplet formation). The analysis did not consider what happened after mass was removed from the jet; i.e. it is not clear what aerodynamic forces (relative velocities) are present once material has left the surface.

Another possibility for the discrepancy is the existence of other jet breakup mechanisms, such as those mentioned earlier and discussed in more detail by Reitz [9]. If the jet does not adhere to the nozzle walls, it could perhaps be more stable than the theory predicts. More detailed analysis of flow in the nozzle (currently under investigation by others) might clear up this concern. Consideration of flow being rearranged as it enters the combustion chamber would perhaps lead to more destabilizing results, although the fact that the fluid is adjoined by a surface on one side could suggest further stabilization.

There is also the likelihood that the input data, particularly relative velocities and annulus area (position of the piston) are in error. A complete set of experimental data does not exist and is certainly not repeatable at present. Any output from a gun code will be questionable until this occurs and verification takes place. "Inverse codes" that use experimental data are somewhat more reliable, but a careful error analysis of all data and subsequent exhaustive computer runs covering all possibilities are required to obtain complete confidence in results.

A related explanation is that unaccounted for energy losses could reduce the liquid accumulation predicted by the inverse code. It is assumed that the pressure rise results from combustion of the liquid with no energy losses. More liquid could burn with energy being lost due to heat transfer.

When evaluating the above, some possibilities appear more likely than others, although the magnitude of error cannot be determined without further study. The most useful exercise would be to conduct conclusive repetitive experiments with reliable data. However, this is the most difficult and expensive suggestion. Based on a rather exhaustive body of literature, and the likelihood that at least velocities are well predicted by the code, it seems probable that aerodynamic forces do strip liquid from the jet as predicted. It is not at all clear, however, what happens next. Perhaps droplets are not formed and, if they are, their size is hard to determine with any accuracy. Coalescence due to interaction among particles or adherence to surfaces is also possible. Another possibility which is easier to check is the existence of substantial energy losses that would reduce the amount of liquid accumulated in the inverse code.

There is clearly much work to be done, but perhaps the above analysis has helped to somehow enhance our understanding of the breakup of liquid monopropellant jets.

TABLE 1. VARIABLE TABULATION FOR GUN DATA

Time m.s.	$\frac{L}{2a}$	$\frac{\rho_2}{\rho_1}$	$\text{Re} \times 10^{-4}$	$\text{We}_1 \times 10^{-4}$	$\text{We}_2 \times 10^{-4}$	Oh	$\frac{\rho_1}{\rho_2} \left( \frac{\sigma}{\mu_1 U_0} \right)^2$	$\text{Log}_{10} \mu_1 / \mu_{H_2O}$
.2	5.54	.013	1.90	14.9	.20	.0203	1.2397	.946
.4	5.26	.022	3.23	40.9	.92	.0196	.2792	.946
.6	4.91	.035	4.71	80.6	2.81	.0191	.0978	.946
.8	4.90	.050	6.01	130.3	6.49	.0190	.0427	.946
1.0	4.90	.065	7.34	193.2	12.60	.0189	.0222	.946
1.2	4.85	.076	8.38	248.0	18.97	.0188	.0149	.946
1.4	4.48	.085	8.12	215.3	18.35	.0181	.0167	.946
1.6	4.03	.092	9.03	238.9	22.01	.0171	.0155	.946
1.8	3.51	.101	10.42	276.4	27.88	.0160	.0141	.946
2.0	2.96	.112	12.37	328.1	36.74	.0146	.0127	.946
2.2	2.89	.123	15.28	486.5	59.78	.0144	.0080	.946
2.4	2.89	.131	17.11	607.6	79.81	.0144	.0060	.946
2.6	2.89	.136	17.64	644.4	87.55	.0144	.0055	.946
2.8	2.89	.137	17.75	651.9	89.38	.0144	.0054	.946
3.0	2.89	.136	17.67	646.6	88.16	.0144	.0055	.946

TABLE 2. ATOMIZATION PREDICTIONS USING  
THE CONTINUOUS MODEL

<u>Time</u>	<u>Mass Left</u>	<u>Jet Length</u>	<u>Mass Atom.</u>	<u>Surface Area</u>
6.15	0.0490	0.1151	0.0400	18.98
6.20	0.0799	0.1808	0.0982	44.93
6.25	0.0992	0.2164	0.1684	74.84
6.30	0.1127	0.2376	0.2457	106.67
6.35	0.1230	0.2545	0.3280	139.96
6.40	0.1292	0.2638	0.4141	174.60
6.45	0.1356	0.2740	0.5037	210.82
6.50	0.1390	0.2807	0.5967	248.92
6.55	0.1424	0.2876	0.6986	298.06
6.60	0.1478	0.2984	0.8220	382.93
6.65	0.1456	0.2902	0.9732	540.93
6.70	0.1411	0.2812	1.1531	830.56
6.75	0.1430	0.2810	1.3477	1214.35
6.80	0.1535	0.2903	1.5601	1709.12
6.85	0.1612	0.2984	1.7939	2337.59
6.90	0.1747	0.3128	2.0506	3115.51
6.95	0.1875	0.3257	2.3298	4047.82
7.00	0.2007	0.3359	2.6303	5134.89
7.05	0.2123	0.3447	2.9476	6324.28
7.10	0.2257	0.3559	3.2701	7485.80
7.15	0.2397	0.3628	3.5949	8603.88
7.20	0.2393	0.3491	3.9325	9833.57
7.25	0.2384	0.3366	4.2799	11261.07
7.30	0.2456	0.3383	4.6200	12615.46
7.35	0.2574	0.3421	4.9594	13922.19
7.40	0.2677	0.3484	5.3001	15193.36
7.45	0.2796	0.3529	5.6429	16435.98
7.50	0.2924	0.3606	5.9885	17652.54
7.55	0.3089	0.3694	6.3483	18970.00
7.60	0.3359	0.3878	6.7480	20667.38
7.65	0.3452	0.3900	7.1985	22932.20
7.70	0.3593	0.3923	7.7030	26055.22
7.75	0.3776	0.4008	8.2409	29712.64
7.80	0.4071	0.4160	8.8182	33955.67
7.85	0.4207	0.4159	9.4480	39136.31
7.90	0.4455	0.4191	10.1270	45496.38
7.95	0.4827	0.4342	10.8407	52494.75
8.00	0.5244	0.4519	11.5963	60203.61
8.05	0.5437	0.4539	12.4061	69026.13
8.10	0.5843	0.4664	13.3149	80860.73
8.15	0.6368	0.4859	14.3131	95341.89
8.20	0.7162	0.5138	15.4083	112671.40
8.25	0.7615	0.5233	16.6209	134052.50
8.30	0.8366	0.5388	17.9474	160528.90
8.35	0.8823	0.5510	19.3589	190107.10
8.40	0.9486	0.5900	20.8876	224487.50
8.45	0.9507	0.5913	22.5692	267729.40
8.50	0.9443	0.5873	24.3774	321690.50
8.55	0.9575	0.5955	26.2804	384149.70
8.60	0.9437	0.5869	28.3386	461050.10

**TABLE 3. ATOMIZATION AND BURNING RATE PREDICTIONS  
USING THE DISCRETE MODEL**

<u>Time</u>	<u>Atomization</u>			<u>Burning</u>		
	<u>Mass Atom.</u>	<u>Mass Left</u>	<u>Jet Length</u>	<u>Mass Burned</u>	<u>Mass Left</u>	<u>Mass In</u>
6.15	0.0338	0.0539	0.1105	0.0000935	0.0876	0.0877
6.20	0.0985	0.0779	0.2175	0.0002776	0.1761	0.1764
6.25	0.1810	0.0850	0.2114	0.0005505	0.2655	0.2660
6.30	0.2662	0.0910	0.2072	0.0009105	0.3563	0.3572
6.35	0.3538	0.0960	0.2048	0.0013570	0.4485	0.4498
6.40	0.4410	0.1028	0.3068	0.0018899	0.5420	0.5439
6.45	0.5319	0.1076	0.3065	0.0025123	0.6370	0.6395
6.50	0.6266	0.1100	0.3083	0.0032268	0.7334	0.7366
6.55	0.7372	0.1090	0.3234	0.0040439	0.8422	0.8462
6.60	0.8721	0.1067	0.2587	0.0049862	0.9738	0.9788
6.65	1.0386	0.0962	0.3071	0.0060781	1.1288	1.1348
6.70	1.2409	0.0726	0.1880	0.0073420	1.3062	1.3135
6.75	1.4422	0.0715	0.2090	0.0087941	1.5049	1.5137
6.80	1.6649	0.0725	0.2285	0.0104519	1.7270	1.7374
6.85	1.9103	0.0751	0.2461	0.0123342	1.9731	1.9855
6.90	2.1789	0.0780	0.2618	0.0144587	2.2424	2.2569
6.95	2.4690	0.0815	0.2756	0.0168338	2.5337	2.5505
7.00	2.7794	0.0877	0.2874	0.0194695	2.8476	2.8671
7.05	3.0981	0.0997	0.2889	0.0223722	3.1754	3.1978
7.10	3.4180	0.1120	0.2813	0.0255337	3.5044	3.5300
7.15	3.7404	0.1234	0.2743	0.0289488	3.8348	3.8633
7.20	4.0783	0.1230	0.2679	0.0326128	4.1687	4.2013
7.25	4.4186	0.1240	0.2619	0.0365214	4.5061	4.5426
7.30	4.7514	0.1343	0.2562	0.0406747	4.8450	4.8857
7.35	5.0869	0.1439	0.2510	0.0450702	5.1858	5.2308
7.40	5.4253	0.1531	0.2462	0.0497022	5.5286	5.5783
7.45	5.7667	0.1618	0.2420	0.0545678	5.8740	5.9285
7.50	6.1114	0.1702	0.2380	0.0596757	6.2219	6.2816
7.55	6.4789	0.1799	0.2482	0.0650272	6.5937	6.6588
7.60	6.8905	0.1924	0.2714	0.0706453	7.0122	7.0829
7.65	7.3609	0.1919	0.2927	0.0765591	7.4762	7.5528
7.70	7.8777	0.1894	0.3119	0.0828009	7.9842	8.0670
7.75	8.4247	0.2016	0.3291	0.0893850	8.5369	8.6263
7.80	9.0140	0.2172	0.3443	0.0963163	9.1348	9.2312
7.85	9.6618	0.2209	0.3576	0.1036224	9.7790	9.8826
7.90	10.3539	0.2277	0.3691	0.1113253	10.4703	10.5816
7.95	11.0755	0.2511	0.3790	0.1194201	11.2072	11.3266
8.00	11.8398	0.2759	0.3873	0.1279144	11.9878	12.1158
8.05	12.6984	0.2848	0.4084	0.1368446	12.8464	12.9832
8.10	13.6709	0.2903	0.4408	0.1462460	13.8149	13.9612
8.15	14.7288	0.3176	0.4692	0.1561203	14.8903	15.0464
8.20	15.8860	0.3560	0.4938	0.1665039	16.0756	16.2421
8.25	17.1688	0.3791	0.5146	0.1774464	17.3705	17.5480
8.30	18.5547	0.4053	0.5321	0.1889534	18.7711	18.9600
8.35	20.0157	0.4621	0.5466	0.2010231	20.2769	20.4779
8.40	21.6219	0.4809	0.5717	0.2137051	21.8891	22.1028
8.45	23.4150	0.4192	0.6092	0.2270412	23.6072	23.8342
8.50	25.3274	0.3454	0.6469	0.2410622	25.4317	25.6728
8.55	27.3489	0.2860	0.6904	0.2558193	27.3791	27.6349
8.60	29.5691	0.1680	0.7397	0.2713833	29.4657	29.7371

# REGIMES FOR JET BREAKUP

FIGURE 1

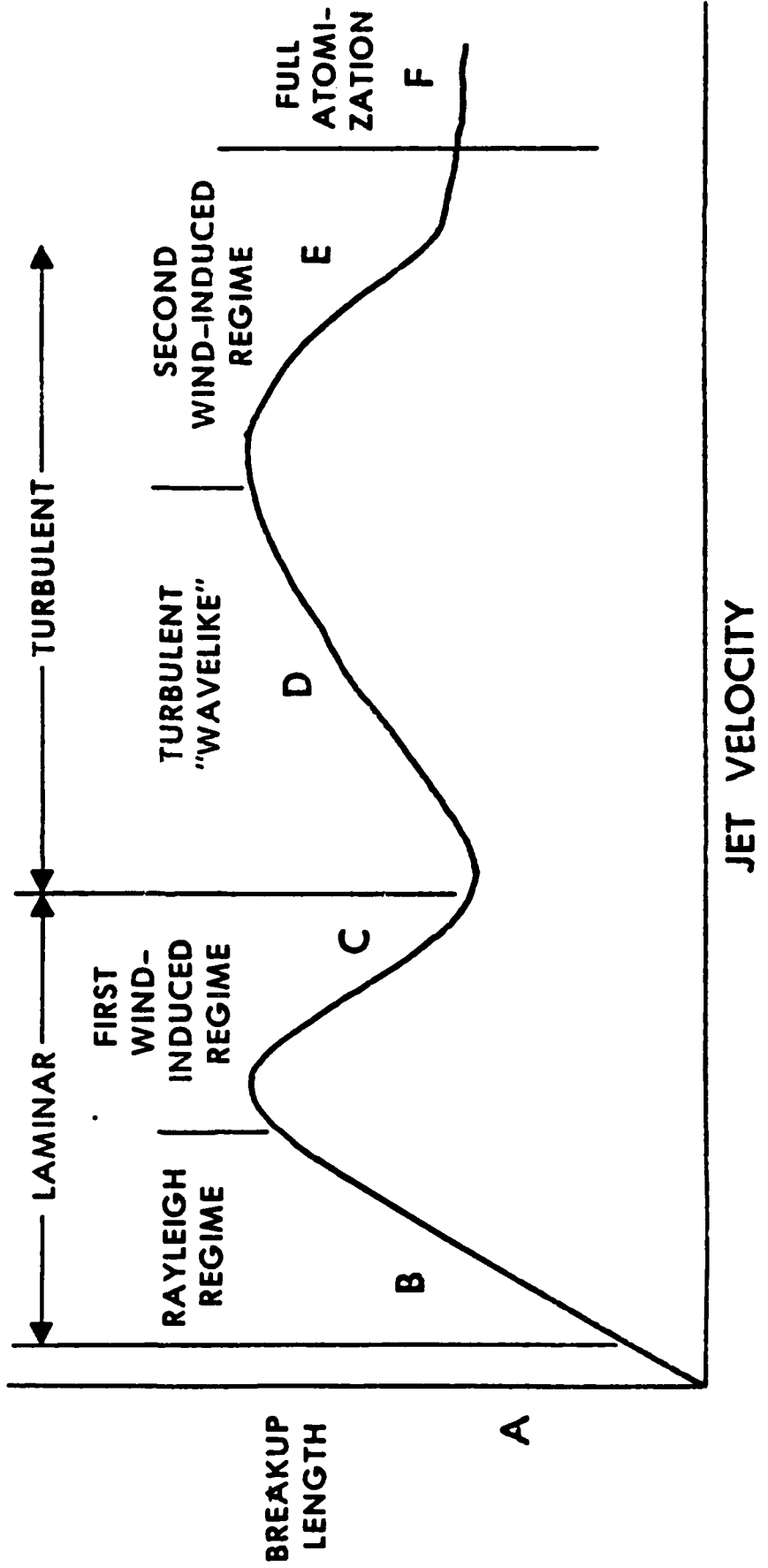
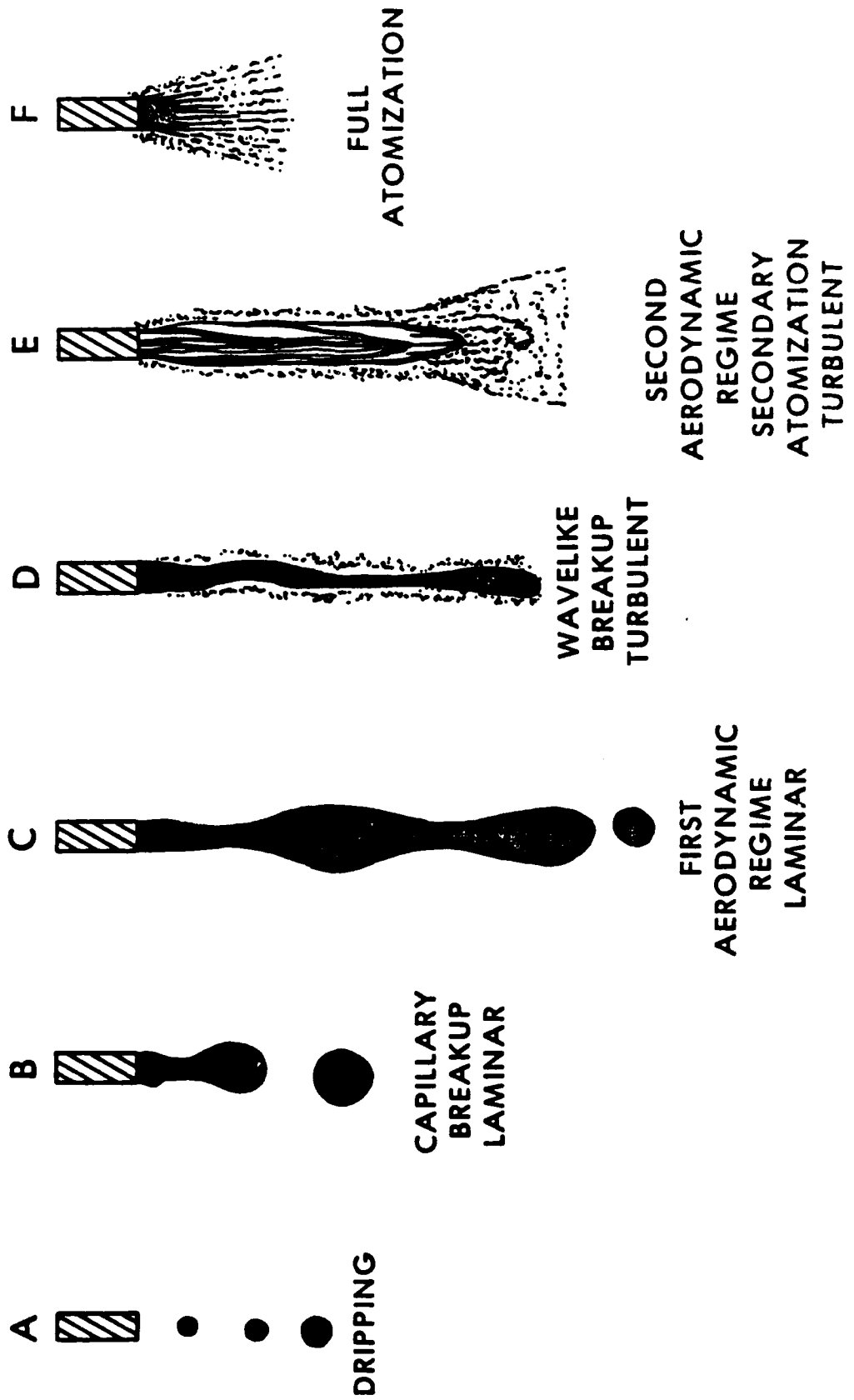


FIGURE 2

# QUALITATIVE PICTURE OF JET BREAKUP



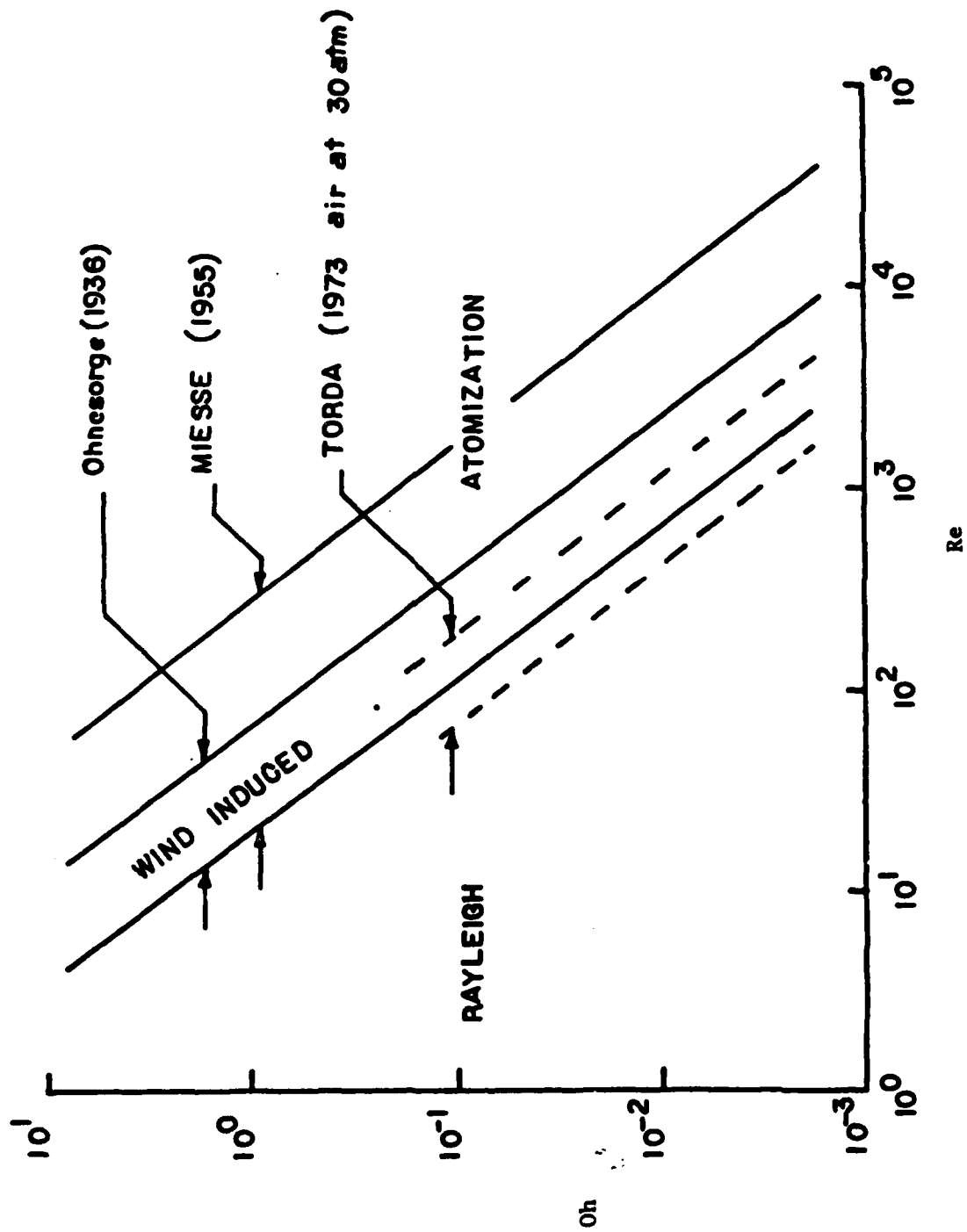


FIGURE 3. JET BREAKUP REGIME BOUNDARIES [9]

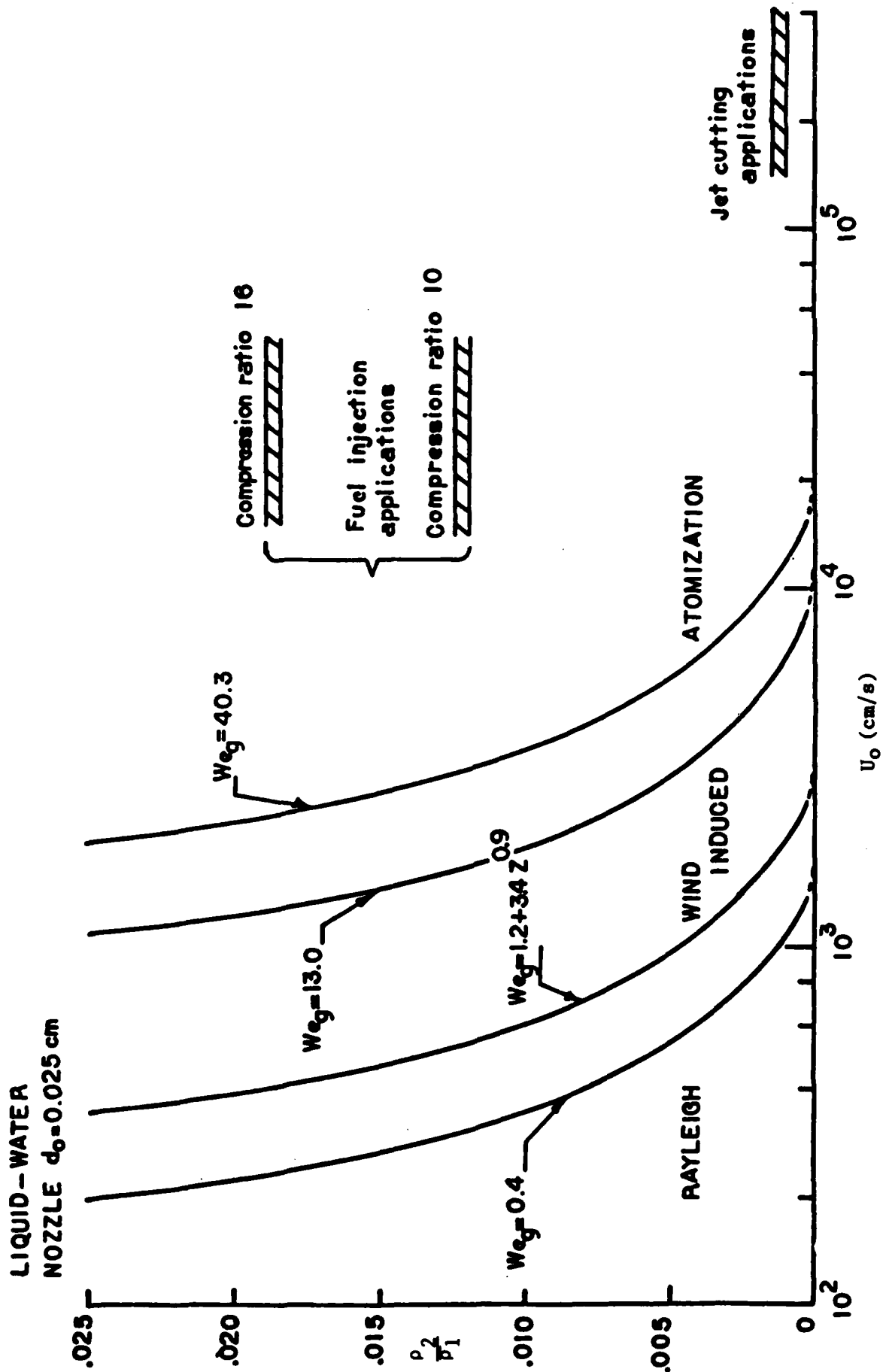


FIGURE 4.

EFFECT OF GAS DENSITY ON JET BREAKUP REGIME BOUNDARIES [9]

FIGURE 5

# SPRAY ANGLE VS DENSITY RATIO

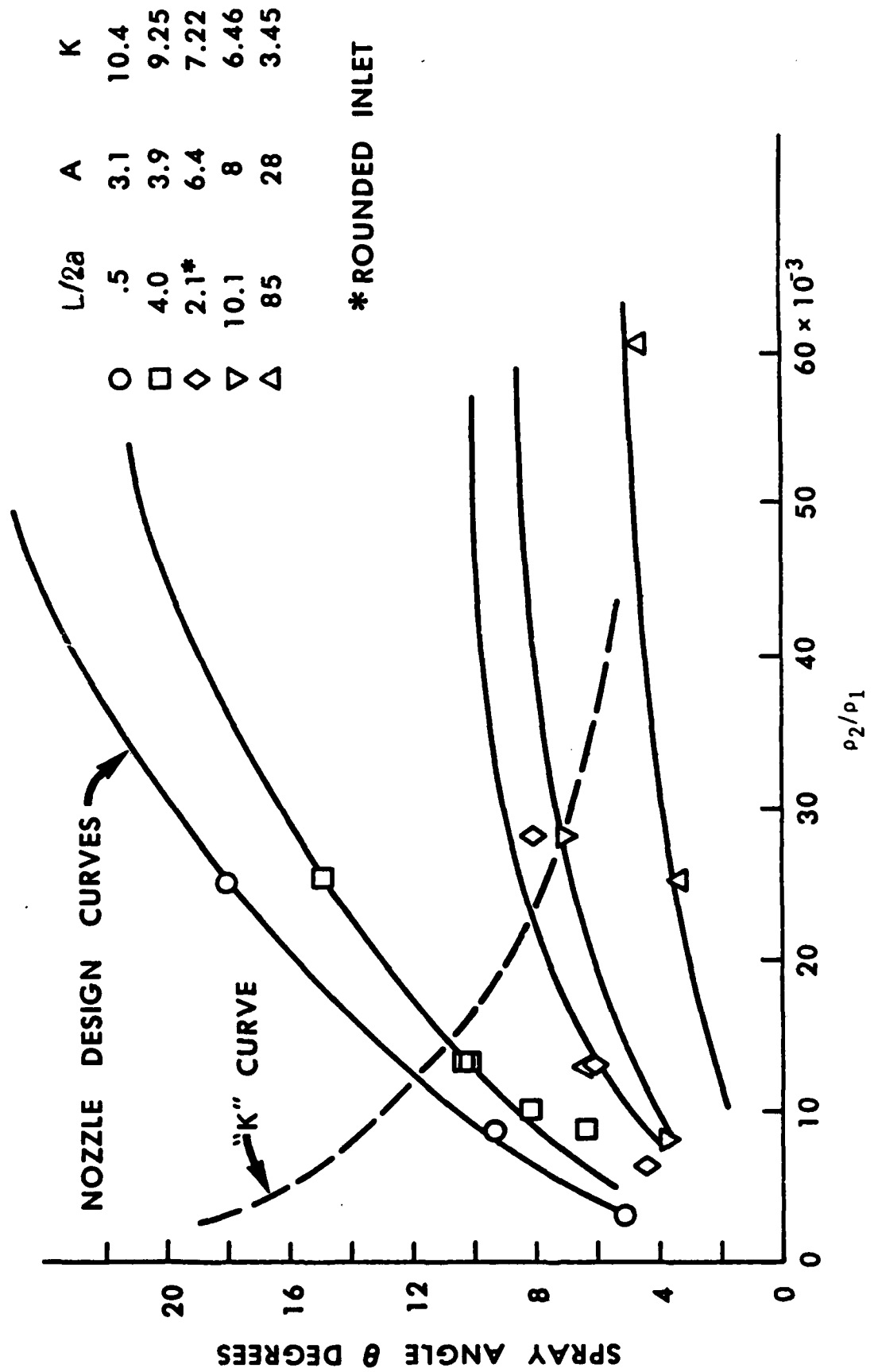
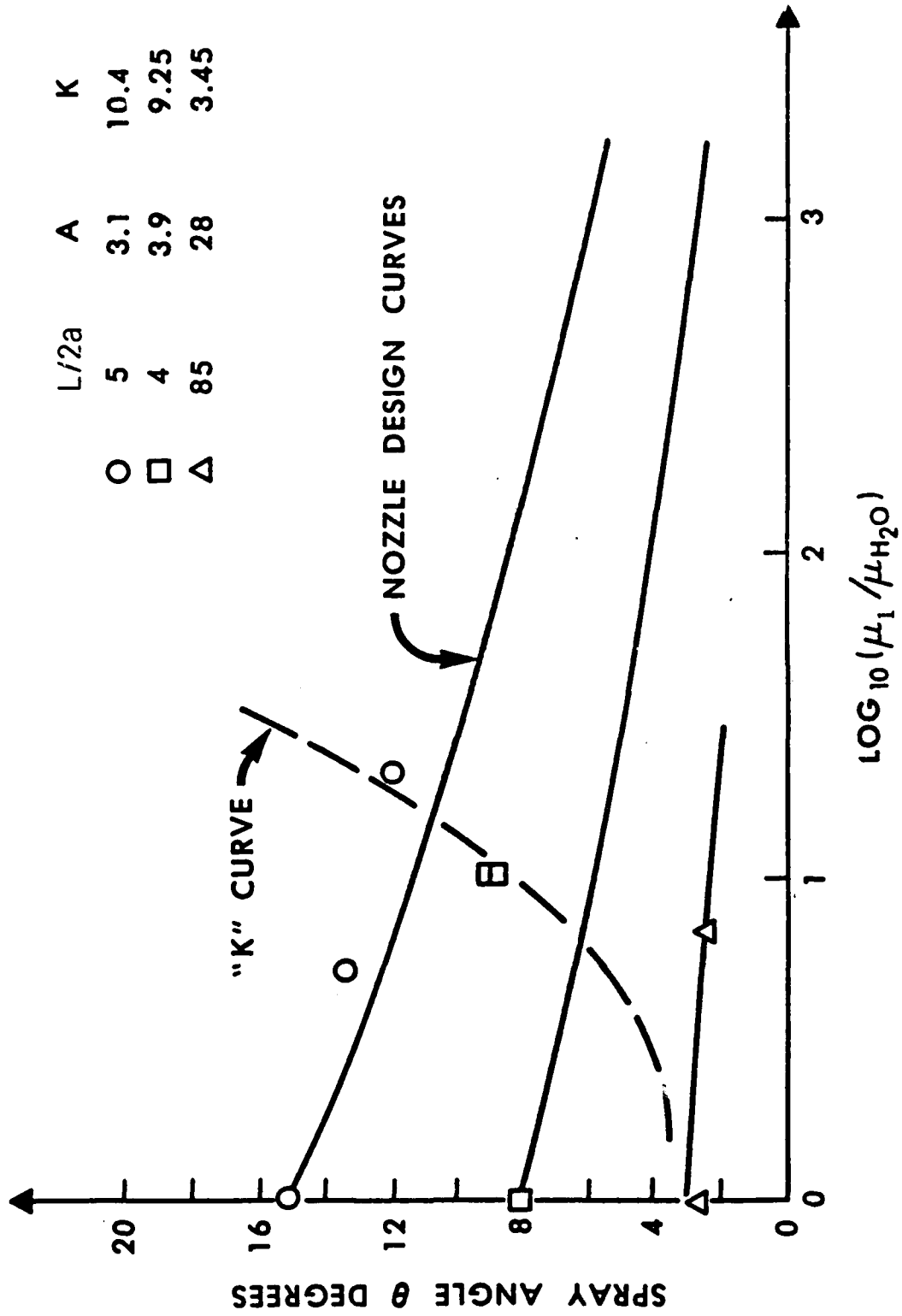


FIGURE 6

# SPRAY ANGLE VS VISCOSITY



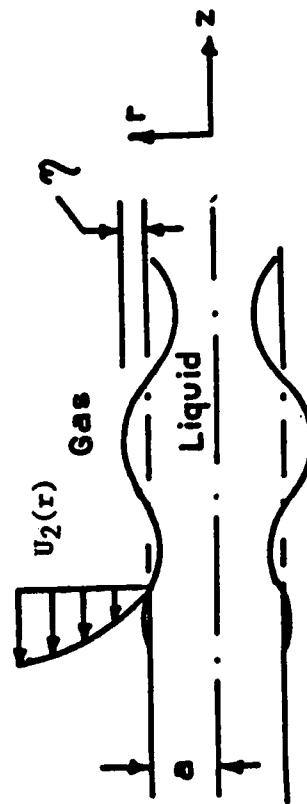


FIGURE 7. FLOW FIELD FOR STABILITY ANALYSIS

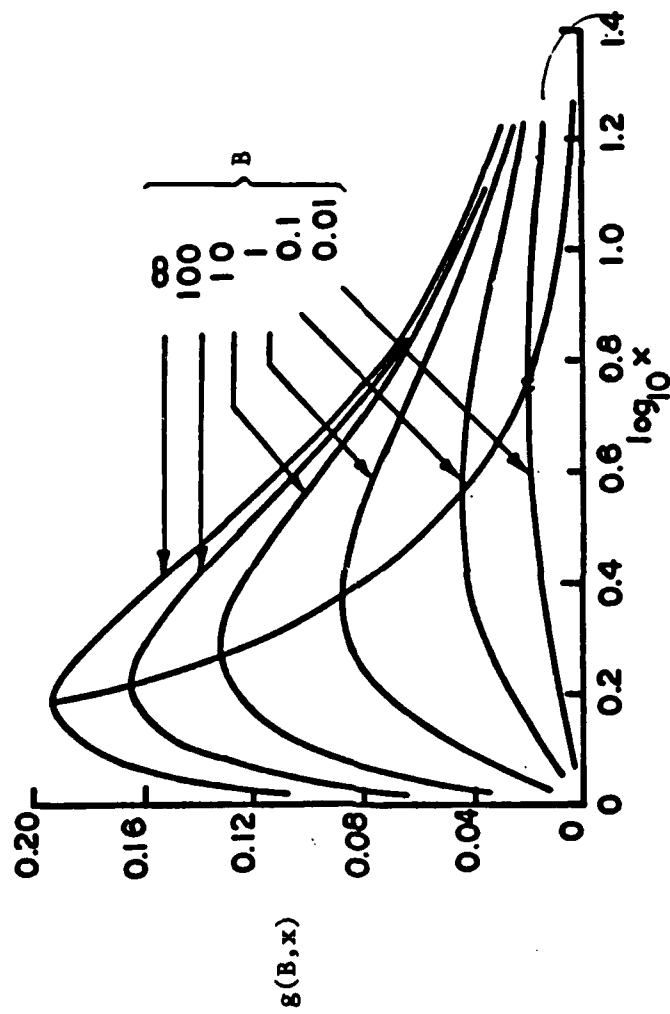


FIGURE 8. DISPERSION RELATION FOR SECOND WIND INDUCED BREAKUP [9]

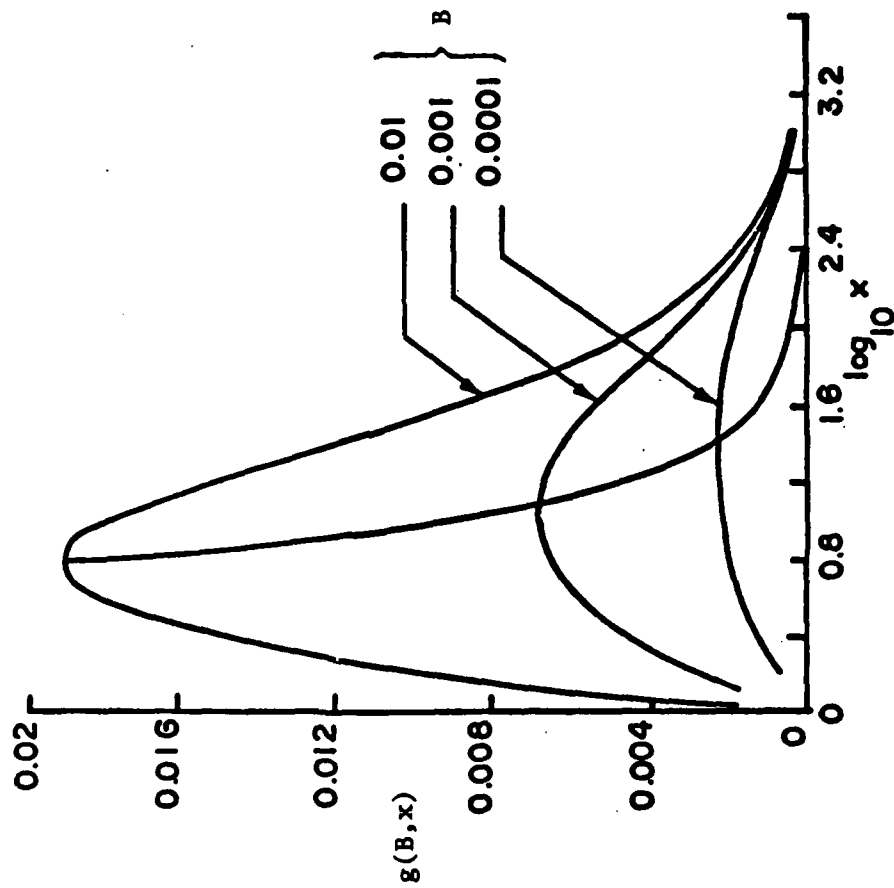


FIGURE 9. DISPERSION RELATION FOR SECOND WIND INDUCED BREAKUP [9]

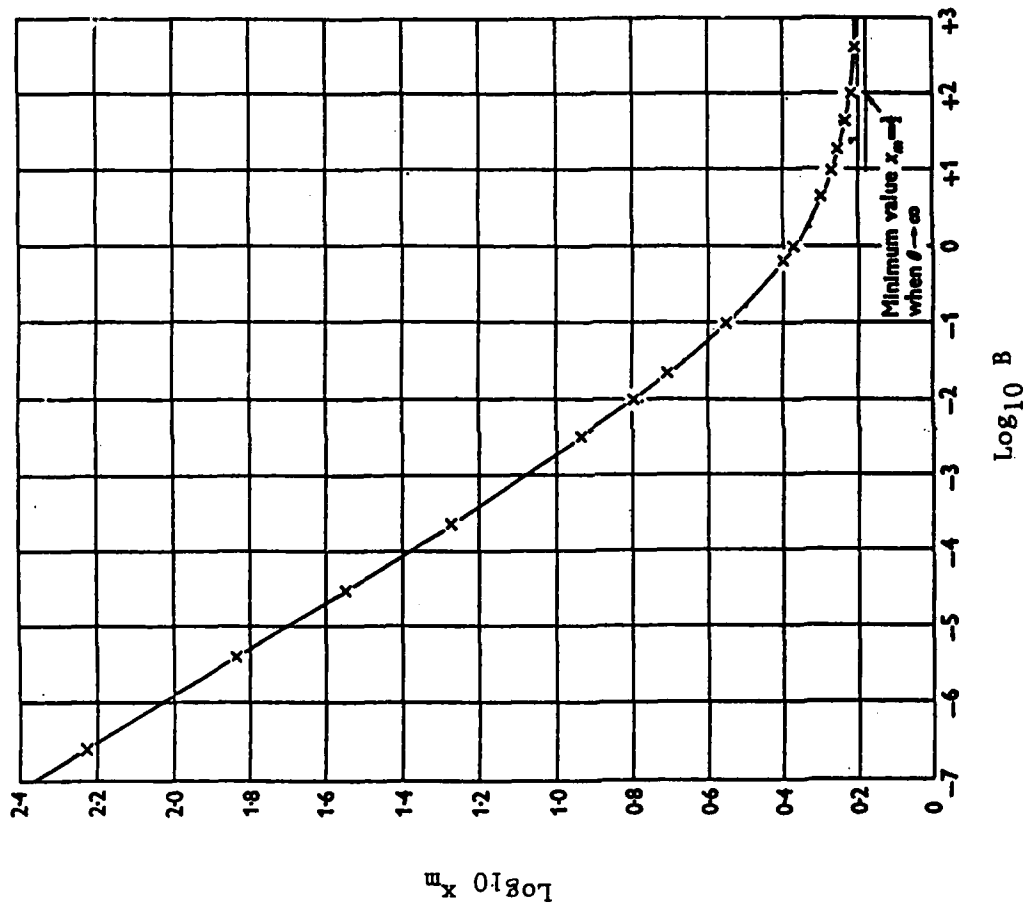


FIGURE 10. LOCUS OF MAXIMUM POINTS OF FIGURES 8 AND 9 [12]

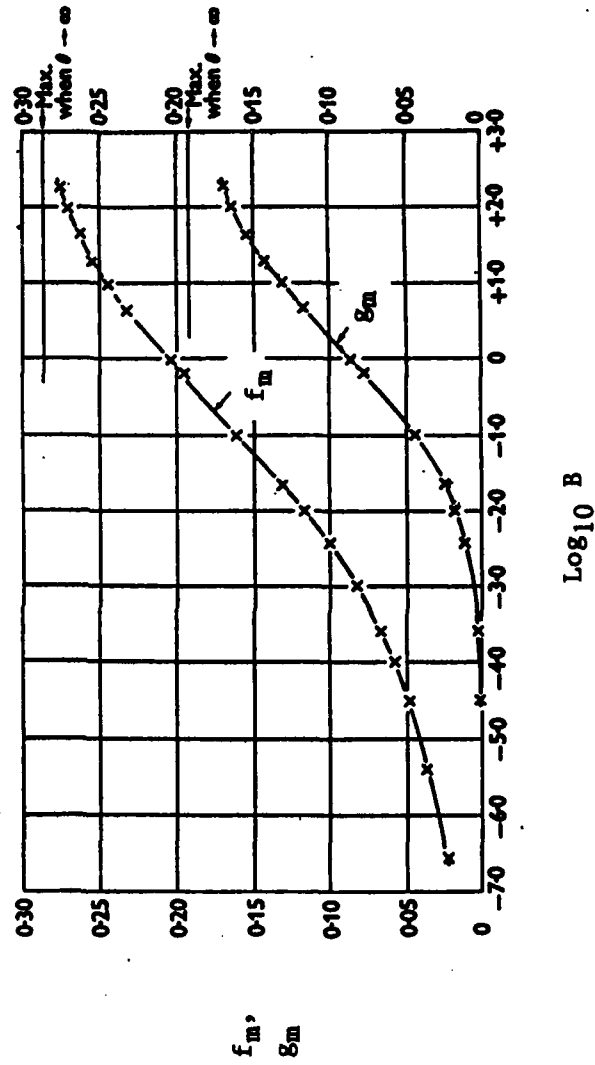
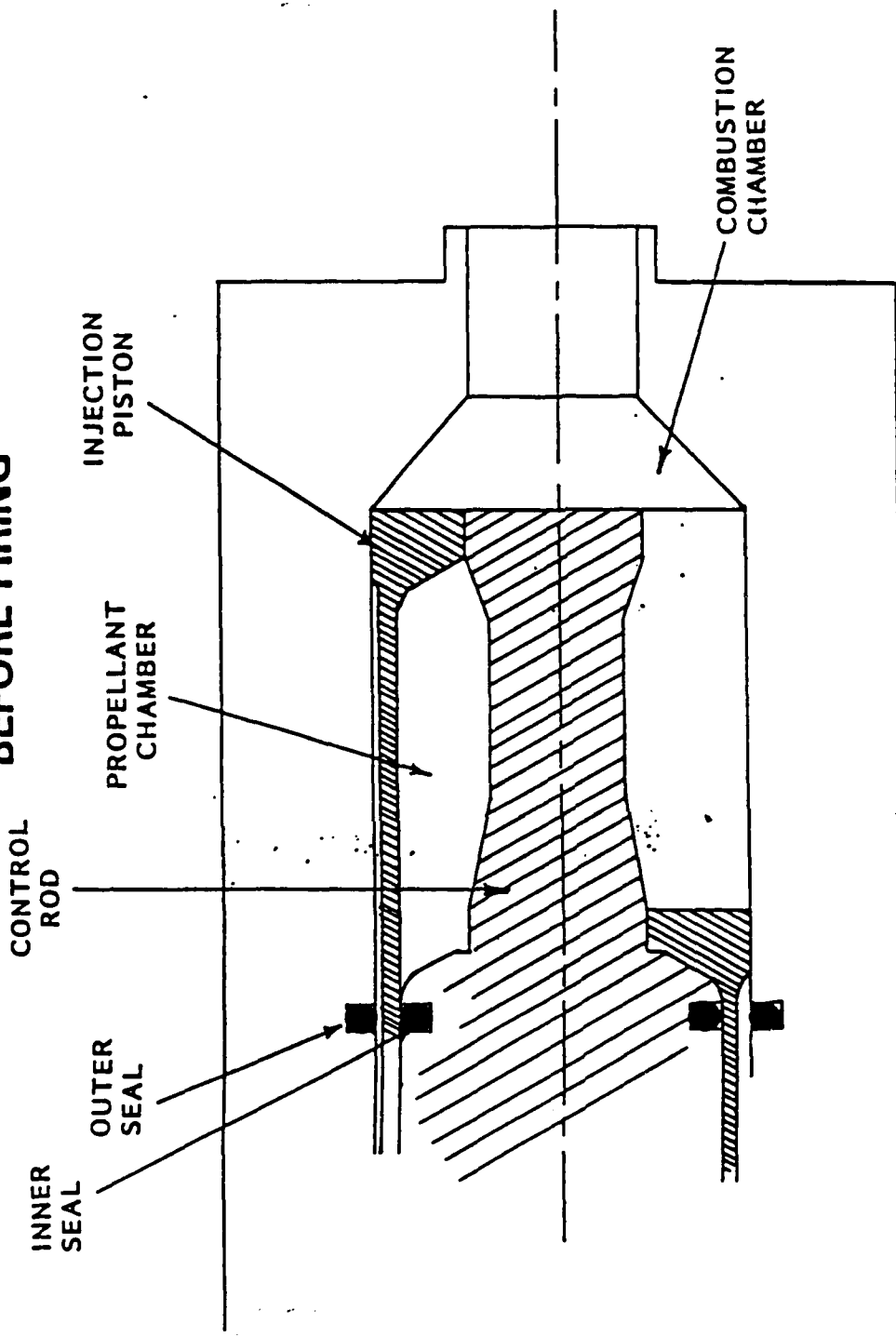


FIGURE 11.  $f_m$  AND  $g_m$  VS.  $\text{LOG}_{10} B$  [12]

**BEFORE FIRING**



**AFTER FIRING**

Figure 12. A Regenerative Liquid Propellant Gun with an Annular Piston [13]

## REFERENCES

- 1 Rayleigh, J. W. S., "Instability of Jets", Proceedings of the London Mathematical Society, Vol. 10 (1878).
- 2 Haenlein, A., "Disintegration of a Liquid Jet", NACA, TN 659 (1932).
- 3 Weber, C. Z., Angew. Math. Mech., 11, 136 (1931).
- 4 Grant, R. P. and Middleman, S., "Newtonian Jet Stability", AIChE Journal, Vol. 12, No. 4, pp. 669-678 (1966).
- 5 Pilcher, J. M. and Miesse, C. C., "The Mechanism of Atomization", WADC, TR 56-344.
- 6 Miesse, C. C., "Correlation of Experimental Data on the Disintegration of Liquid Jets", Indust. Engng. Chem., Vol. 47, p. 1690 (1955).
- 7 Ranz, W. E., "Some Experiments on Orifice Sprays", The Canadian Journal of Chemical Engineering, Vol. 36, p. 175 (1958).
- 8 Sterling, A. M. and Sleicher, C. A., "The Instability of Capillary Jets", Journal of Fluid Mechanics, Vol. 68, p. 477 (1975).
- 9 Reitz, R. D., Atomization and Other Breakup Regimes of a Liquid Jet, PhD Dissertation, Princeton University (1978).
- 10 Reitz, R. D. and Bracco, F. V., "On the Dependence of Spray Angle and Other Spray Parameters on Nozzle Design and Operating Conditions", SAE Paper No. 790494 (1979).
- 11 Levich, V. G., Physicochemical Hydrodynamics, pp. 639-652, Prentice-Hall (1962).
- 12 Taylor, G. I., "Generation of Ripples by Wind Blowing over a Viscous Fluid", The Scientific Papers of G. I. Taylor, Vol. III, edited by G. K. Batchelor, Cambridge University Press, pp. 244-254.
- 13 Coffee, T. P., "A Lumped Parameter Code for Regenerative Liquid Propellant Guns", Technical report BRL-TR-2703 (1985).
- 14 Coffee, T. P., "The Analysis of Experimental Measurements on Liquid Regenerative Guns", Technical Report BRL-TR-2731 (1986).

## NOMENCLATURE

- a - jet radius
- A - constant, equations (12) and (13), Chapter 2
- B - droplet formation parameter,  $\rho_1/\rho_2 \left(\frac{\sigma}{u_1 U_0}\right)^2$
- C, C<sub>1</sub>, C<sub>2</sub>, C<sub>3</sub> - constants
- d - drop diameter
- D - annulus outer diameter
- f - function, equation (30), Chapter 3
- g - function, equation (17), Chapter 3
- k - disturbance wave number,  $2\pi/\lambda$
- l - wave parameter, equation (12), Chapter 3
- L - length of nozzle
- l - intact length of jet
- m - mass
- $\dot{m}$  - mass removed per unit surface area and time
- p - pressure
- r - direction perpendicular to axis
- t - time
- u - fluctuating (perturbation) velocity in z direction (parallel to jet axis)
- U<sub>0</sub> - relative velocity of the liquid, U<sub>1</sub> - U<sub>2</sub>
- U<sub>1</sub> - axial velocity profile in the liquid
- U<sub>2</sub> - axial velocity profile in the gas
- v - fluctuating (perturbation) velocity in r direction (perpendicular to jet axis)
- V - velocity of gas or liquid in axial z direction
- x - wavelength parameter,  $\rho_2 U_0^2/\sigma k$
- z - direction parallel to axis

### Nomenclature (continued)

- $\delta$  = annulus thickness
- $\lambda$  = disturbance wavelength
- $\eta$  = surface wave elevation (r direction)
- $\nu$  = kinematic viscosity
- $\mu$  = absolute viscosity
- $\sigma$  = surface tension
- $\omega$  = disturbance growth rate (1/time)
- $\phi$  = velocity potential
- $\psi$  = stream function
- $\theta$  = spray angle

### Subscripts

- i = component
- 1 = liquid component
- 2 = gas component
- o = jet (at nozzle exit)
- m = maximum value, value corresponding to drop formation

APPENDIX A

Computer Programs

```

C PROGRAM TO CALCULATE THE AMOUNT OF LIQUID THAT IS ATOMIZED IN AN ANNULUS
C PROGRAM NAME IS JETC.FTN.THIS VERSION ALSO CALCULATES DROP SIZE DISTRIBUTION.
C WRITTEN BY NELSON MACKEN OCT.86.REVISED 21 DEC TO ALSO COMPUTE BURNING RATE.
C
C IN THIS PROGRAM,DIMENSIONS ARE VAR(J,I),WHERE J TRACKS LUMP OF MASS THAT
C LEFT INLET AT TIME T(J),AND I REPRESENTS CURRENT TIME.
C
C DIMENSION T(60),V(60),VI(60),VP(60),AV(60),DEL(60),
1 RHOL(60),RHOG(60),SDR(60,60),SDRT(60),BRATE(60),
2 BAREA(60),PRESS(60),TTMBUR(0:60),TTMLEB(0:60)
REAL L(60),LNET(60),MIN(60),MNET(0:60),MREMO(60,60),
1 MREMA(0:60,0:60),MATOM(60),MINNET,MNETT,LNETT,MDR,
2 LM(60,60),MLEFTB(0:60,0:60),MBURN(60,60)
REAL NDRJT,NDR(60,60),NDRT(60),NDRNET,MINTT(60)
INTEGER LL(60),LBURN(60)

C
C OPEN(10,FILE='CONST.JETC',STATUS='OLD')
C OPEN(20,FILE='OUTPUT.JETC',STATUS='NEW')
C
C PI=3.1416
C DT=.05E-3
C ST=71.6
C VISL=.08935
C DB=1.7
C
C N=51
100 FORMAT(7(F7.2,2X))
READ(10,100)(T(I),VI(I),VP(I),AV(I),RHOL(I),RHOG(I),
1 PRESS(I),I=1,N)
C WRITE(20,100)(T(I),VI(I),VP(I),AV(I),RHOL(I),
C 1 RHOG(I),PRESS(I),I=1,N)
C
C RESET DATA SO USE AVERAGES FOR EACH TIMESTEP.
C
C N=50
DO 170 I=1,N
T(I)=T(I+1)
V(I)=(VI(I)+VI(I+1))/2.
AV(I)=(AV(I)+AV(I+1))/2.
RHOL(I)=(RHOL(I)+RHOL(I+1))/2.
RHOG(I)=(RHOG(I)+RHOG(I+1))/2.
170 PRESS(I)=(PRESS(I)+PRESS(I+1))/2.

C
C DO 110 I=1,N
C L(I)=V(I)*DT
C MIN(I)=AV(I)*V(I)*RHOL(I)*DT
110 CONTINUE
C
C 120 FORMAT(2X,F4.2,2X,F6.1,2X,F5.3,2X,F8.5)
C WRITE(20,120)(T(I),V(I),DEL(I),B(I),I=1,N)
C

```

```

LLL=2
IF(LLL.EQ.1) GO TO 500
DO 150 I=1,N
150 LL(I)=0
MINNET=0.
SDRNET=0.
NDRNET=0
C ***** PRINT TITLE FOR OUTPUT *****
C PRINT*,''
C PRINT*, '**** DROP SIZE DISTRIBUTION *****'
DO 130 I=1,N
C PRINT*, ' TIME= ',T(I)
MREMA(I,I-1)=MIN(I)
MNETT=0.
LNETT=0.
NDRTT=0
SDRTT=0.
DO 140 J=1,I
IF(LL(J).NE.1) THEN
  B=(RHOL(J)/RHOG(J))*(ST/(VISL*V(I)))**2.
  XP=LOG10(B)
  IF(XP.LE.-5.) F=.01*XP+.09
  IF(XP.GT.-5..AND.XP.LE.-3.) F=.02*XP+.14
  IF(XP.GT.-3..AND.XP.LE.-1.) F=.0375*XP+.1925
  IF(XP.GT.-1..AND.XP.LE.1.) F=.045*XP+.2
  IF(XP.GT.1) F=.0175*XP+.2275
  IF(XP.LE.-2.) XM=10.**(-.29*XP+.22)
  IF(XP.GT.-2..AND.XP.LE.-1.) XM=10.**(-.24*XP+.32)
  IF(XP.GT.-1..AND.XP.LE.0.) XM=10.**(-.185*XP+.375)
  IF(XP.GT.0..AND.XP.LE.1.) XM=10.**(-.095*XP+.375)
  IF(XP.GT.1..AND.XP.LE.2.) XM=10.**(-.05*XP+.33)
  IF(XP.GT.2.) XM=10.**(-.03*XP+.29)
  LM(J,I)=2.*PI*ST*XM/(RHOG(J)*V(I)**2.)
  MDR=RHOL(J)*PI*LM(J,I)**3./6.
  ADR=PI*LM(J,I)**2.
  MREMO(J,I)=4.*PI**2.*DB*(RHOG(J)/RHOL(J))**.5*RHOL(J)*F
1 *V(I)*L(J)*DT
MREMA(J,I)=MREMA(J,I-1)-MREMO(J,I)
IF(MREMA(J,I).LE.0.) THEN
  MREMO(J,I)=MREMA(J,I-1)
  MREMA(J,I)=0.
  L(J)=0.
  LL(J)=1
END IF
MNETT=MNETT+MREMA(J,I)
LNETT=LNETT+L(J)
NDR(J,I)=MREMO(J,I)/MDR
SDR(J,I)=NDR(J,I)*ADR
NDRTT=NDRTT+NDR(J,I)
SDRTT=SDRTT+SDR(J,I)
C PRINT*,''
C PRINT*, ' TIME OF MASS INJECTION= ',T(J)
C PRINT*, ' MASS IN DROP FORM= ',MREMO(J,I)
C PRINT*, ' DROP DIAMETER= ',LM(J,I)
C PRINT*, ' NUMBER OF DROPS= ',NDR(J,I)

```

```

C      PRINT*, ' SURFACE AREA OF DROPS= ',SDR(J,I)
      END IF
140  CONTINUE
      MNET(I)=MNETT
      LNET(I)=LNETT
      MINNET=MINNET+MIN(I)
      MATOM(I)=MINNET-MNET(I)
      SDRT(I)=SDRTT
      NDRT(I)=NDRTT
      NDRNET=NDRNET+NDRT(I)
      SDRNET=SDRNET+SDRT(I)
C      PRINT*, '
C      PRINT*, ' NUMBER OF DROPS AT THIS TIME= ',NDRT(I)
C      PRINT*, ' SURFACE AREA AT THIS TIME= ',SDRT(I)
C      PRINT*, '
C      PRINT*, ' TOTAL MASS ATOMIZED= ',MATOM(I)
C      PRINT*, ' TOTAL NUMBER OF DROPS= ',NDRNET
C      PRINT*, ' TOTAL SURFACE AREA= ',SDRNET
C      PRINT*, '
C      PRINT*, '
130  CONTINUE
C
C      THIS PART OF THE PROGRAM WILL CALCULATE THE BURNING RATE AND THE
C      MASS INVENTORY AS IF THERE IS ONLY BURNING OCCURING.
C
500  CONTINUE
      PRINT*, '
C      PRINT*, ' ***** BURNING CALCULATIONS *****'
      DO 180 I=1,N
      LBURN(I)=1
180  BRATE(I)=1.64*PRESS(I)**.103
      MINNET=0.
      DO 182 I=1,N
C      PRINT*, 'TIME=',T(I)
      BAREA(I)=PI*V(I)*DB*DT
      MLEFTB(I,I-1)=MIN(I)
      TMBURN=0.
      TMLEFB=0.
      DO 184 J=1,I
      IF(LBURN(J).NE.0) THEN
          MBURN(J,I)=BAREA(J)*BRATE(I)*RHOL(J)*DT
          MLEFTB(J,I)=MLEFTB(J,I-1)-MBURN(J,I)
          IF(MLEFTB(J,I).LE.0.) THEN
              MBURN(J,I)=MLEFTB(J,I-1)
              MLEFTB(J,I)=0.
              LBURN(J)=0
          END IF
          TMBURN=TMBURN+MBURN(J,I)
          TMLEFB=TMLEFB+MLEFTB(J,I)
      END IF
184  CONTINUE
      MINNET=MINNET+MIN(I)
      MINTT(I)=MINNET
      TTMLEB(I)=TMLEFB
      TTMBUR(I)=MINNET-TMLEFB

```

```
C      PRINT*,'  
C      PRINT*,'TOTAL MASS BURNED AT THIS TIME      ',TTMBUR(I)  
C      PRINT*,'TOTAL MASS NOT BURNED AT THIS TIME',TTMLEB(I)  
182  CONTINUE  
  
C  
C      PRINT OUT SUMMARY DATA  
C  
      WRITE(20,188)  
      WRITE(20,186)(T(I),MATOM(I),MNET(I),LNET(I),TTMBUR(I),  
1  TTMLEB(I),MINTT(I),I=1,N)  
188  FORMAT(////)  
186  FORMAT(2X,F4.2,2X,F7.4,2X,F7.4,2X,F7.4,2X,F10.7,2X,  
1  F7.4,2X,F7.4)  
      CLOSE(10)  
      CLOSE(20)  
      END
```

```

C *****
C
C PROGRAM TO CALCULATE THE AMOUNT OF LIQUID THAT IS ATOMIZED IN AN ANNULUS
C PROGRAM NAME IS JETC.FTN.THIS VERSION THIS VERSION USES ODE SOLVER "EPISODE"
C WRITTEN BY NELSON MACKEN 31 DEC 86
C
C *****
C *****
C ***** MAIN PROGRAM SETS UP ODE SOLVER *****
C *****
C
C DEFINITION OF VARIABLES
C
C Y(1)=V(I) VELOCITY OF JET
C Y(2)=AV(I) AREA OF DRIFICE
C Y(3)=RHOG(I) DENSITY OF GAS IN COMBUSTION CHAMBER
C Y(4)=RHOL(I) DENSITY OF LIQUID ENTERING COMBUSTION CHAMBER
C Y(5)=MIN(I) TOTAL MASS THAT HAS ENTERED COMBUSTION CHAMBER
C Y(6)=MATOM TOTAL MASS THAT HAS BEEN ATOMIZED
C Y(7)=SURF TOTAL SURFACE AREA OF DROPLETS THAT HAVE BEEN ATOMIZED
C
C DIMENSION T(60),PRESS(60),Y(10),VP(60)
C COMMON/VAR/VI(60),AV(60),RHOL(60),RHOG(60)
C COMMON/CONST/I,DT
C COMMON/OUTPUT/AMLEF,ALEN
C
C OPEN(10,FILE='CONST.JETC',STATUS='OLD')
C OPEN(20,FILE='OUTPUT.JETC',STATUS='NEW')
C
C N=51
C READ(10,100)(T(I),VI(I),VP(I),AV(I),RHOL(I),RHOG(I),
1 PRESS(I),I=1,N)
C WRITE(20,100)(T(I),VI(I),VP(I),AV(I),RHOL(I),
1 RHOG(I),PRESS(I),I=1,N)
C
C PARAMETERS FOR DRIVE
C NI=7
C HO=1.E-10
C EPS=1.E-4
C IERROR=3
C MF=10
C INDEX=1
C INITIALIZE VARIABLES
C Y(1)=VI(1)
C Y(2)=AV(1)
C Y(3)=RHOG(1)
C Y(4)=RHOL(1)
C Y(5)=0.
C Y(6)=0.
C Y(7)=0.

```

```

XO=6.1E-3
WRITE(20,300)
DT=.05E-3
XOUT=XO+DT
C SET UP LOOP TO SOLVE
N=51
DO 2 I=2,N
CALL DRIVE(NI,XO,HO,Y,XOUT,EPS,IERROR,MF,INDEX)
IF(INDEX.NE.0) STOP
WRITE(20,200)T(I),AMLEF,ALEN,Y(6),Y(7)
XOUT=XOUT+DT
2 CONTINUE
CLOSE(10)
CLOSE(20)
C
100 FOF:MAT(7(F7.2,2X))
200 FORMAT(10X,F4.2,5X,F6.4,5X,F6.4,5X,F7.4,5X,F9.2)
300 FORMAT(//)
C
END
C
END OF MAIN PROGRAM
C
*****
C ** SUBROUTINE VARC COMPUTES PROPERTIES AT INTERMEDIATE TIME STEPS **
C *****
C
SUBROUTINE VARC(YD1,YD2,YD3,YD4)
COMMON/VAR/VI(60),AV(60),RHOL(60),RHOG(60)
COMMON/CONST/I,DT
C
DEFINITIONS OF DERIVATIVES
C
YD1= D(VELOCITY)/DT
YD2= D(AREA)/DT
YD3= D(RHOG)/DT
YD4= D(RHOL)/DT
C
YD1=(VI(I)-VI(I-1))/DT
YD2=(AV(I)-AV(I-1))/DT
YD3=(RHOG(I)-RHOG(I-1))/DT
YD4=(RHOL(I)-RHOL(I-1))/DT
C
RETURN
END
C
END OF SUBROUTINE VARC
C
*****
C ** SUBROUTINE ATOM COMPUTES PARAMETERS FOR ATOMIZATION ****
C

```

```

C *****
C
C   SUBROUTINE ATOM(V,AV,RHOG,RHOL,Y5,Y6,YD5,YD6,YD7)
C
C   COMMON/OUTPUT/AMLEF,ALEN
C   REAL MDR,LM,MLEFT,LEN
C
C   DEFINITIONS OF VARIABLES
C
C   V= JET VELOCITY,CM/SEC
C   AV= VENT(ORIFICE) AREA,CM**2
C   RHOG= GAS DENSITY,GM/CM**3
C   RHOL= LIQUID DENSITY,GM/CM**3
C   FLIN= TOTAL MASS THAT HAS ENTERED COMBUSTION CHAMBER,GM
C   PI= VALUE OF "PI"
C   ST= SURFACE TENSION,GM/SEC**2
C   VISL= LIQUID VISCOSITY,GM/CM-SEC
C   DB= DIAMETER OF BOLT,CM
C   B,XP,F= DROPLET FORMATION PARAMETERS
C   LM= WAVELENGTH OF DETACHED FLUID,DIAMETER OF DROPLET,CM
C   MDR= MASS OF DROPLET,GM
C   ADR= AREA OF DROPLET,CM**2
C   MLEFT,AMLEF= MASS REMAINING IN LIQUID CORE,GM
C   LEN,ALEN= LENGTH OF LIQUID CORE,CM
C   R1,R2= RADII OF FRUSTRUM FORMED BY LIQUID CORE,CM
C   SURFA= OUTER SURFACE OF FRUSTRUM (LIQUID CORE)
C   Y(5),Y5= TOTAL MASS THAT HAS ENTERED THE COMBUSTION CHAMBER,GM
C   Y(6),Y6= TOTAL MASS THAT HAS BEEN ATOMIZED,GM
C   Y(7)= TOTAL SURFACE AREA OF ATOMIZED LIQUID,CM**2
C   YD5= MASS FLOW INTO THE COMBUSTION CHAMBER,GM/SEC
C   YD6= YDOT(6)
C   YD7= YDOT(7)
C
C   CONSTANTS
C
C   PI=3.1416
C   ST=71.6
C   VISL=.08935
C   DB=1.7
C
C   CALCULATE THE MASS FLOW INTO THE COMBUSTION CHAMBER
C
C   YD5=RHOL*AV*V
C
C   VARIABLES FOR THE CALCULATION OF THE MASS ATOMIZED
C
C   B=(RHOL/RHOG)*(ST/(VISL*V))**2.
C   XP=LOG10(B)
C   IF(XP.LE.-5.)           F=.01*XP+.09
C   IF(XP.GT.-5..AND.XP.LE.-3.) F=.02*XP+.14
C   IF(XP.GT.-3..AND.XP.LE.-1.) F=.0375*XP+.1925
C   IF(XP.GT.-1..AND.XP.LE.1.)  F=.045*XP+.2
C   IF(XP.GT.1)             F=.0175*XP+.2275
C   IF(XP.LE.-2.)          XM=10.**(-.29*XP+.22)
C   IF(XP.GT.-2..AND.XP.LE.-1.) XM=10.**(-.24*XP+.32)

```

```

IF(XP.GT.-1..AND.XP.LE.0.) XM=10.**(-.185*XP+.375)
IF(XP.GT.0..AND.XP.LE.1.) XM=10.**(-.095*XP+.375)
IF(XP.GT.1..AND.XP.LE.2.) XM=10.**(-.05*XP+.33)
IF(XP.GT.2.) XM=10.**(-.03*XP+.29)
LM=2.*PI*ST*XM/(RHOG*V**2.)
MDR=RHOL*PI*LM**3./6.
ADR=PI*LM**2.

```

```

C
C CALCULATE THE SURFACE AREA REMAINING THAT IS NOT ATOMIZED,
C ASSUMING MASS LEFT FORMS A "HOLLOW" FRUSTRUM WITH CURRENT
C VALUES FOR THE LIQUID DENSITY.
C

```

```

R1=DB/2.+AV/(PI*DB)
R2=DB/2.
MLEFT=Y5-Y6
LEN=MLEFT/(RHOL*PI*(1./3.*(R1**2.+R1*R2+R2**2.)-
1R2**2.))
SURFA=PI*(R1+R2)*(LEN**2.+(R1-R2)**2.）**.5

```

```

C
C CALCULATE MASS ATOMIZED PER UNIT TIME
C

```

```

YD6=4.*PI*RHOL*V*(RHOG/RHOL)**.5*F*SURFA

```

```

C
C CALCULATE SURFACE AREA INCREASE PER UNIT TIME
C

```

```

YD7=YD6*ADR/MDR

```

```

C
C SAVE MASS LEFT AND JET LENGTH FOR OUTPUT
C

```

```

AMLEF=MLEFT
ALEN=LEN

```

```

C
C RETURN
C END

```

```

C
C END OF SUBROUTINE ATOM
C

```

```

C *****
C

```

```

C *** SUBROUTINE DIFFUN IS CALLED BY ODE SOLVER *****
C

```

```

C *****
C

```

```

SUBROUTINE DIFFUN(N,XOUT,Y,YDOT)

```

```

C
C DIMENSION Y(N),YDOT(N)
C

```

```

GATHER VALUES OF VELOCITY,AREA,DENSITYS

```

```

C
C CALL VARC(YDOT(1),YDOT(2),YDOT(3),YDOT(4))
C

```

```

GATHER THE MASS ATOMIZED AND THE SURFACE AREA ATOMIZED

```

```

C
C CALL ATOM(Y(1),Y(2),Y(3),Y(4),Y(5),Y(6),YDOT(5),YDOT(6)
1,YDOT(7))

```

```
C
  RETURN
  END
C
  END OF SUBROUTINE DIFFUN
C *****
C
C ***** END OF PROGRAM JETC - ODE SOLVER TO BE BINDED TO RUN ****
C
C *****
```

DISTRIBUTION LIST

<u>No. of</u> <u>Copies</u>	<u>Organization</u>	<u>No. of</u> <u>Copies</u>	<u>Organization</u>
12	Commander Defense Technical Info Center ATTN: DTIC-DDA Cameron Station Alexandria, VA 22304-6145	3	Director Benet Weapons Laboratory Armament R&D Center US Army AMCCOM ATTN: SMCAR-LCB-TL E. Conroy A. Graham Watervliet, NY 12189
1	Director Defense Advanced Research Projects Agency ATTN: H. Fair 1400 Wilson Boulevard Arlington, VA 22209	1	Commander US Army Armament, Munitions and Chemical Command ATTN: SMCAR-ESP-L Rock Island, IL 61299-7300
1	HQDA DAMA-ART-M Washington, DC 20310	1	Commander US Army Aviation Research and Development Command ATTN: AMSAV-E 4300 Goodfellow Blvd. St. Louis, MO 63120
1	Commander US Army Materiel Command ATTN: AMCDRA-ST 5001 Eisenhower Avenue Alexandria, VA 22333-0001	1	Commander Materials Technology Lab US Army Laboratory Cmd ATTN: SLCMT-MCM-SB M. Levy Watertown, MA 02172-0001
13	Commander Armament R&D Center US Army AMCCOM ATTN: SMCAR-TSS SMCAR-TDC SMCAR-SCA, B. Brodman R. Yalamanchili SMCAR-LCA, D. Downs A. Beardell SMCAR-LCE, N. Slagg SMCAR-LCS, W. Quine A. Bracuti J. Lannon SMCAR-FSS-A, R. Price L. Frauen SMCAR-FSA-S, H. Liberman Picatinny Arsenal, NJ 07806-5000	1	Director US Army Air Mobility Rsch. and Development Lab. Ames Research Center Moffett Field, CA 94035
		1	Commander US Army Communications Electronics Command ATTN: AMSEL-ED Fort Monmouth, NJ 07703
		1	Commander ERADCOM Technical Library ATTN: STET-L Ft. Monmouth, NJ 07703-5301

DISTRIBUTION LIST

<u>No. of Copies</u>	<u>Organization</u>	<u>No. of Copies</u>	<u>Organization</u>
1	Commander US Army Harry Diamond Labs ATTN: DELHD-TA-L 2800 Powder Mill Rd Adelphi, MD 20783	1	Commander Armament Rsch & Dev Ctr US Army Armament, Munitions and Chemical Command ATTN: SMCAR-CCS-C, T Hung Picatinny Arsenal, NJ 07806-5000
1	Commander US Army Missile Command Rsch, Dev, & Engr Ctr ATTN: AMSMI-RD Redstone Arsenal, AL 35898	1	Commandant US Army Field Artillery School ATTN: ATSF-CMW Ft Sill, OK 73503
1	Commander US Army Missile & Space Intelligence Center ATTN: AIAMS-YDL Redstone Arsenal, AL 35898-5500	1	Commandant US Army Armor Center ATTN: ATSB-CD-MLD Ft Knox, KY 40121
1	Commander US Army Belvoir R&D Ctr ATTN: STRBE-WC Tech Library (Vault) B-315 Fort Belvoir, VA 22060-5606	1	Commander US Army Development and Employment Agency ATTN: MODE-TED-SAB Fort Lewis, WA 98433
1	Commander US Army Tank Automotive Cmd ATTN: AMSTA-TSL Warren, MI 48397-5000	1	Commander Naval Surface Weapons Center ATTN: D.A. Wilson, Code G31 Dahlgren, VA 22448-5000
1	Commander US Army Research Office ATTN: Tech Library P.O. Box 12211 Research Triangle Park, NC 27709-2211	1	Commander Naval Surface Weapons Center ATTN: Code G33, J. East Dahlgren, VA 22448-5000
1	Director US Army TRADOC Systems Analysis Activity ATTN: ATAA-SL White Sands Missile Range NM 88002	2	Commander US Naval Surface Weapons Ctr. ATTN: O. Dengel K. Thorsted Silver Spring, MD 20902-5000
1	Commandant US Army Infantry School ATTN: ATSH-CD-CSO-OR Fort Benning, GA 31905	1	Commander Naval Weapons Center China Lake, CA 93555-6001
1	Commandant US Army Infantry School ATTN: ATSH-CD-CSO-OR Fort Benning, GA 31905	1	Commander Naval Ordnance Station ATTN: C. Dale Code 5251 Indian Head, MD 20640

DISTRIBUTION LIST

<u>No. of Copies</u>	<u>Organization</u>	<u>No. of Copies</u>	<u>Organization</u>
1	Superintendent Naval Postgraduate School Dept of Mechanical Eng. ATTN: Code 1424, Library Monterey, CA 93943	10	Central Intelligence Agency Office of Central Reference Dissemination Branch Room GE-47 HQS Washington, DC 20502
1	AFWL/SUL Kirtland AFB, NW 87117	1	Central Intelligence Agency ATTN: Joseph E. Backofen HQ Room 5F22 Washington, DC 20505
1	Air Force Armament Lab ATTN: AFATL/DLODL Eglin, AFB, FL 32542-5000	4	Bell Aerospace Textron ATTN: F. Boorady K. Berman A.J. Friona J. Rockenfeller Post Office Box One Buffalo, NY 14240
1	AFOSR/NA (L. Caveny) Bldg. 410 Bolling AFB, DC 20332	1	Calspan Corporation ATTN: Tech Library P.O. Box 400 Buffalo, NY 14225
1	Commandant USAFAS ATTN: ATSF-TSM-CN Ft Sill, OK 73503-5600	7	General Electric Ord. Sys Dpt ATTN: J. Mandzy, OP43-220 R.E. Mayer H. West M. Bulman R. Pate I. Magoon W. O'Connor 100 Plastics Avenue Pittsfield, MA 01201-3698
1	Director Jet Propulsion Lab ATTN: Tech Libr 4800 Oak Grove Drive Pasadena, CA 91109	1	General Electric Company Armanent Systems Department ATTN: D. Maher Burlington, VT 05401
2	Director National Aeronautics and Space Administration ATTN: MS-603, Tech Lib MS-86, Dr. Povinelli 21000 Brookpark Road Lewis Research Center Cleveland, OH 44135	1	IITRI ATTN: Library 10 W. 35th St. Chicago, IL 60616
1	Director National Aeronautics and Space Administration Manned Spacecraft Center Houston, TX 77058	1	Olin Chemicals Research ATTN: David Gavin P.O. Box 586 Cheshire, CT 06410-0586

DISTRIBUTION LIST

<u>No. of Copies</u>	<u>Organization</u>	<u>No. of Copies</u>	<u>Organization</u>
2	Olin Corporation ATTN: Victor A. Corso Dr. Ronald L. Dotson P.O. Box 30-9644 New Haven, CT 06536	2	University of Delaware Department of Chemistry ATTN: Mr. James Cronin Professor Thomas Brill Newark, DE 19711
1	Paul Gough Associates ATTN: Paul Gough PO Box 1614 Portsmouth, NH 03801	1	U. of ILLinois at Chicago ATTN: Professor Sohail Murad Dept of Chemical Eng Box 4348 Chicago, IL 60680
1	Safety Consulting Engr ATTN: Mr. C. James Dahn 5240 Pearl St. Rosemont, IL 60018	1	U. of Maryland at College Park ATTN: Professor Franz Kasler Department of Chemistry College Park, MD 20742
1	Science Applications, Inc. ATTN: R. Edelman 23146 Cumorah Crest Woodland Hills, CA 91364	1	U. of Missouri at Columbia ATTN: Professor R. Thompson Department of Chemistry Columbia, MO 65211
1	Sunstrand Aviation Operations ATTN: Dr. Owen Briles P.O. Box 7002 Rockford, IL 61125	1	U. of Michigan ATTN: Prof. Gerard M. Faeth Department of Aerospace Engineering Ann Arbor, MI 48109-3796
1	Veritay Technology, Inc. ATTN: E. B. Fisher 4845 Millersport Highway, P.O. Box 305 East Amherst, NY 14051-0305	1	U. of Missouri at Columbia ATTN: Professor F. K. Ross Research Reactor Columbia, MO 65211
1	Director Applied Physics Laboratory The Johns Hopkins Univ. Johns Hopkins Road Laurel, Md 20707	1	U. of Missouri at Kansas City Department of Physics ATTN: Prof. R.D. Murphy 1110 East 48th Street Kansas City, MO 64110-2499
2	Director Chemical Propulsion Info Agency The Johns Hopkins Univ. ATTN: T. Christian Tech Lib Johns Hopkins Road Laurel, MD 20707	1	Pennsylvania State University Dept. of Mechanical Eng ATTN: K. Kuo University Park, PA 16802

DISTRIBUTION LIST

<u>No. of Copies</u>	<u>Organization</u>	<u>No. of Copies</u>	<u>Organization</u>
2	Princeton Combustion Rsch Laboratories, Inc. ATTN: N.A. Messina M. Summerfield 475 US Highway One North Monmouth Junction, NJ 08852		
1	University of Arkansas Department of Chemical Engineering ATTN: J. Havens 227 Engineering Building Fayetteville, AR 72701		

Aberdeen Proving Ground

Dir, USAMSAA  
ATTN: AMXSU-D  
AMXSU-MP, H. Cohen

Cdr, USATECOM  
ATTN: AMSTE-TO-F

CDR, CRDEC, AMCCOM  
ATTN: SMCCR-RSP-A  
SMCCR-MU  
SMCCR-SPS-IL

USER EVALUATION SHEET/CHANGE OF ADDRESS

This Laboratory undertakes a continuing effort to improve the quality of the reports it publishes. Your comments/answers to the items/questions below will aid us in our efforts.

1. BRL Report Number \_\_\_\_\_ Date of Report \_\_\_\_\_
2. Date Report Received \_\_\_\_\_
3. Does this report satisfy a need? (Comment on purpose, related project, or other area of interest for which the report will be used.) \_\_\_\_\_  
\_\_\_\_\_  
\_\_\_\_\_
4. How specifically, is the report being used? (Information source, design data, procedure, source of ideas, etc.) \_\_\_\_\_  
\_\_\_\_\_  
\_\_\_\_\_
5. Has the information in this report led to any quantitative savings as far as man-hours or dollars saved, operating costs avoided or efficiencies achieved, etc? If so, please elaborate. \_\_\_\_\_  
\_\_\_\_\_  
\_\_\_\_\_
6. General Comments. What do you think should be changed to improve future reports? (Indicate changes to organization, technical content, format, etc.) \_\_\_\_\_  
\_\_\_\_\_  
\_\_\_\_\_

CURRENT ADDRESS

Name \_\_\_\_\_

Organization \_\_\_\_\_

Address \_\_\_\_\_

City, State, Zip \_\_\_\_\_

7. If indicating a Change of Address or Address Correction, please provide the New or Correct Address in Block 6 above and the Old or Incorrect address below.

OLD ADDRESS

Name \_\_\_\_\_

Organization \_\_\_\_\_

Address \_\_\_\_\_

City, State, Zip \_\_\_\_\_

(Remove this sheet, fold as indicated, staple or tape closed, and mail.)

FOLD HERE

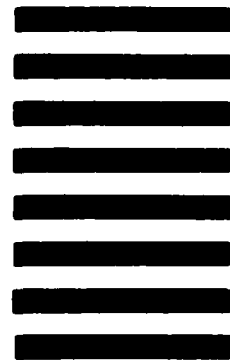
Director  
US Army Ballistic Research Laboratory  
ATTN: DRXBR-OD-ST  
Aberdeen Proving Ground, MD 21005-5066



NO POSTAGE  
NECESSARY  
IF MAILED  
IN THE  
UNITED STATES

OFFICIAL BUSINESS  
PENALTY FOR PRIVATE USE. \$300

**BUSINESS REPLY MAIL**  
FIRST CLASS PERMIT NO 12062 WASHINGTON, DC  
POSTAGE WILL BE PAID BY DEPARTMENT OF THE ARMY



Director  
US Army Ballistic Research Laboratory  
ATTN: DRXBR-OD-ST  
Aberdeen Proving Ground, MD 21005-9989

FOLD HERE